Journal of Medicinal Chemistry

Article

pubs.acs.org/jmc

Discovery of a Selective Kinase Inhibitor (TAK-632) Targeting Pan-RAF Inhibition: Design, Synthesis, and Biological Evaluation of *C*-7-Substituted 1,3-Benzothiazole Derivatives

Masanori Okaniwa,*[,†] Masaaki Hirose,*[,†] Takeo Arita,[†] Masato Yabuki,[†] Akito Nakamura,[†] Terufumi Takagi,[†] Tomohiro Kawamoto,[†] Noriko Uchiyama,[†] Akihiko Sumita,[‡] Shunichirou Tsutsumi,[‡] Tsuneaki Tottori,[‡] Yoshitaka Inui,[†] Bi-Ching Sang,[§] Jason Yano,[§] Kathleen Aertgeerts,[§,∥] Sei Yoshida,[†] and Tomoyasu Ishikawa*[,†]

[†]Pharmaceutical Research Division, Takeda Pharmaceutical Company Limited, 26-1 Muraoka-Higashi 2-chome, Fujisawa, Kanagawa 251-8555, Japan

[‡]CMC Center, Takeda Pharmaceutical Company Limited, 17-85 Jusohonmachi 2-chome, Yodogawa-ku, Osaka 532-8686, Japan

[§]Structural Biology, Takeda California, Inc., 10410 Science Center Drive, San Diego, California 92121, United States

Supporting Information

ABSTRACT: With the aim of discovering a selective kinase inhibitor targeting pan-RAF kinase inhibition, we designed novel 1,3-benzothiazole derivatives based on our thiazolo[5,4-*b*]pyridine class RAF/VEGFR2 inhibitor **1** and developed a regioselective cyclization methodology for the *C*-7-substituted 1,3-benzothiazole scaffold utilizing meta-substituted anilines. Eventually, we selected 7-cyano derivative **8B** (TAK-632) as a development candidate and confirmed its binding mode by cocrystal structure with BRAF. Accommodation of the 7-cyano group into the BRAF-selectivity pocket and the 3-(trifluoromethyl)phenyl acetamide moiety into the hydrophobic back pocket of BRAF in the DFG-out conformation contributed to enhanced RAF potency and selectivity vs VEGFR2. Reflecting its potent pan-RAF inhibition and slow off-rate profile, **8B** demonstrated significant cellular activity against mutated *BRAF* or mutated *NRAS* cancer cell lines. Furthermore, in both A375 ($BRAF^{V600E}$) and HMVII ($NRAS^{Q61K}$) xenograft models in rats, **8B** demonstrated regressive antitumor efficacy by twice daily, 14-day repetitive administration without significant body weight loss.

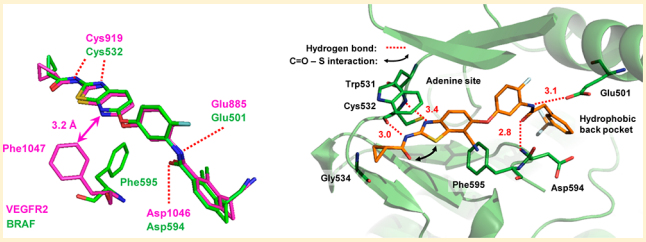

INTRODUCTION

The RAF family of protein kinases plays critical roles in cancer progression.[1] Recently, BRAF selective inhibitors such as vemurafenib (PLX4032)[2−4] and dabrafenib (GSK2118436)[5] have shown significant clinical efficacy in melanoma patients bearing oncogenic $BRAF^{V600E}$ mutation (Figure 1). However, adverse events such as rapid development of squamous cell carcinoma (SCC) and keratoacanthoma have been reported.[3,5−8] These observations were thought to be caused by paradoxical activation of the MAPK pathway by BRAF selective inhibitors in cells bearing wild-type *BRAF* ($BRAF^{wt}$).[9−11] Recent studies[10,12,13] on this paradoxical activation reported that RAF inhibitors instinctively transactivate RAF homodimers (CRAF−CRAF) or heterodimers (CRAF−BRAF(wt)) and activate RAS dependent MAPK signaling. Hence, it has been reported that selective BRAF(V600E) inhibitors, like vemurafenib, have not shown potent antiproliferative activity against cancer cell lines such as *NRAS* mutant melanoma in which RAS dependent MAPK signaling is activated.[14]

To analyze this, our initial investigation (Supporting Information, Table S1) revealed that the feedback activation in fibroblast CsFb cells ($BRAF^{wt}$) was significantly suppressed by our DFG-out type pan-RAF inhibitor, but not by DFG-in type inhibitors, which significantly induced the phosphorylation of downstream MEK and ERK in CsFb cells. On the basis of these results, our interest was directed toward DFG-out type pan-RAF inhibitors to treat cancer patients including oncogenic $BRAF^{V600E}$ as well as *NRAS* mutant in which BRAF (wt) and CRAF are being involved in aberrant signal transduction. Therefore, we initiated a drug discovery program aimed at targeting DFG-out type pan-RAF inhibitors.

We have previously reported potent DFG-out type pan-RAF inhibitors[15−17] and identified the thiazolo[5,4-*b*]pyridine derivative **1** as an inhibitor of RAF and VEGFR2 kinases (BRAF(V600E) IC_{50}, 5.6 nM; BRAF(wt), 12 nM; CRAF, 1.5 nM) and VEGFR2 (2.8 nM) (Figure 1).[15] Compound **1** also showed potent cellular activity such as MAPK signal inhibition in various cell lines possessing the $BRAF^{V600E}$ mutation and VEGFR2 phosphorylation inhibition in 293/KDR cells. In vivo studies in a rat A375 xenograft model demonstrated regressive antitumor efficacy for compound **1** based on dual inhibition of

Received: May 26, 2013

   dx.doi.org/10.1021/jm400778d | *J. Med. Chem.* XXXX, XXX, XXX−XXX

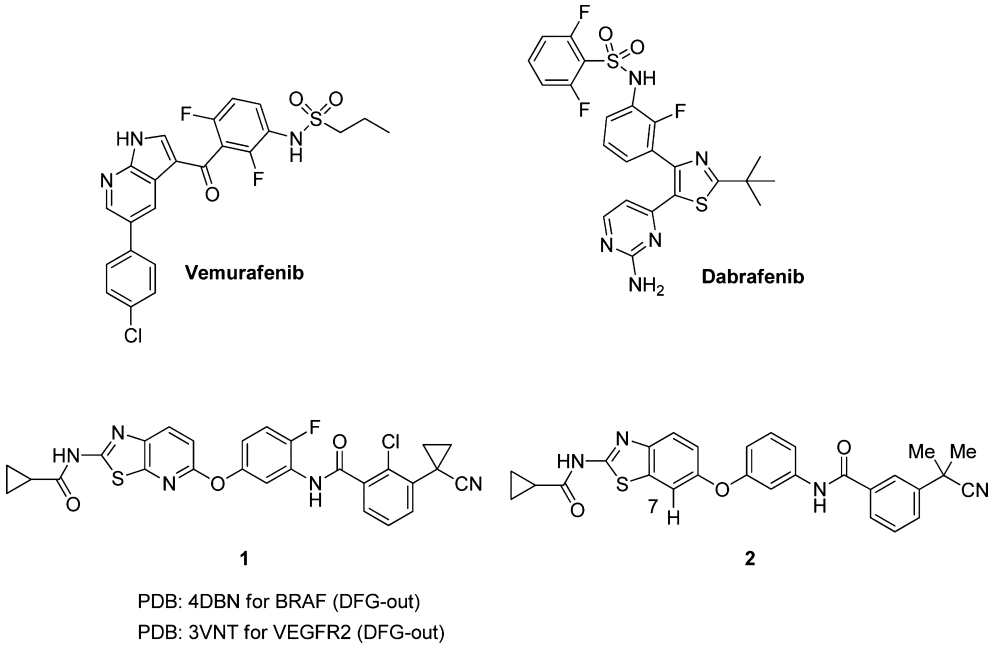

Figure 1. Chemical structures of RAF inhibitors including [1,3]thiazolo[5,4-*b*]pyridine derivative **1** and 1,3-benzothiazole derivative **2** as lead compounds.

RAF and VEGFR2. However, a rat toxicological study of **1** showed pathological changes derived from angiogenesis inhibition but not MAPK inhibition. These results imply that compound **1** could be exerting antiangiogenesis activity on vascular endothelial cells rather than MAPK inhibition on cancer cells. On the basis of these results, we sought to increase the pan-Raf kinase inhibitory potency relative to that for VEGFR2 kinase.

To better understand kinase selectivity, we utilized the X-ray cocrystal structures of compound **1** bound to BRAF (PDB code: 4DBN) and VEGFR2 (PDB code: 3VNT), which we previously reported.[18] The two cocrystal structures were superimposed and analyzed for differences. It was revealed that there is a notable difference between BRAF and VEGFR2 in the conformations of the benzene ring of phenylalanine in the DFG motif (Figure 2). The benzene ring of Phe595 in BRAF (shown in green) is located below the thiazolo[5,4-*b*]pyridine scaffold, whereas that of Phe1047 in VEGFR2 (shown in purple) is located in front of the *N*-7 position of thiazolo[5,4-*b*]pyridine **1** with a distance of 3.2 Å. Consequently, we envisioned that the introduction of a suitable substituent at the *C*-7 position of 1,3-benzothiazole **2**[15] (Figure 1) could reduce VEGFR2 inhibitory activity by steric repulsion between Phe1047 and the 7-substituent (Figures 3 and 4A). On

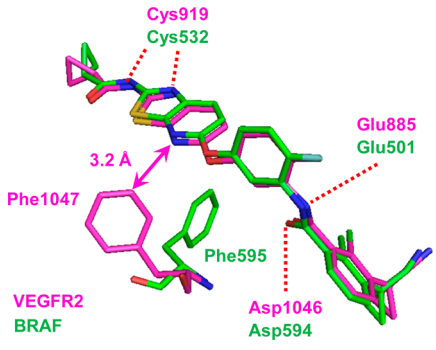

Figure 2. Structural differences in the adenine sites of BRAF and VEGFR2 bound to RAF/VEGFR2 inhibitor **1**. The BRAF structure (4DBN) is shown in green and the VEGFR2 stucture (3VNT) in purple.

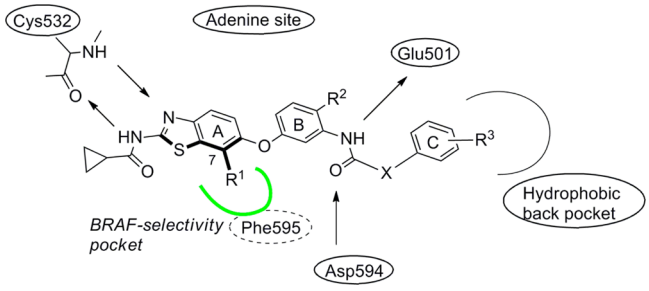

Figure 3. Structure of designed *C*-7-substituted 1,3-benzothiazole derivatives and their predicted binding mode to the DFG-out conformation of BRAF.

the basis of this hypothesis to increase BRAF selectivity over VEGFR2, we planned to introduce an R^1 substituent that would be accommodated in this BRAF-selectivity pocket in front of the *C*-7 position.

Additionally, we examined a new ring B−linker−ring C moiety targeting the hydrophobic back pocket of BRAF (Figures 3 and 4B). According to our crystallographic data, the NHCO amide substructure connected to ring B could apparently form two significant hydrogen bonds with Glu501 and Asp594. Insertion of X (NH or CH_2) into the linker was an important modification because the additional amine (X = NH) of ureides **4**−**6** could form an additional hydrogen bond with the carboxylic acid of Glu501, and the methylene (X = CH_2) of the acetamides **7**−**9** was considered flexible enough that the conformation of ring C could adjust to be accommodated into the hydrophobic back pocket of BRAF.

Our synthetic strategy for the preparation of the *C*-7-substituted 1,3-benzothiazole scaffold is shown in Scheme 1.

dx.doi.org/10.1021/jm400778d | *J. Med. Chem.* XXXX, XXX, XXX−XXX

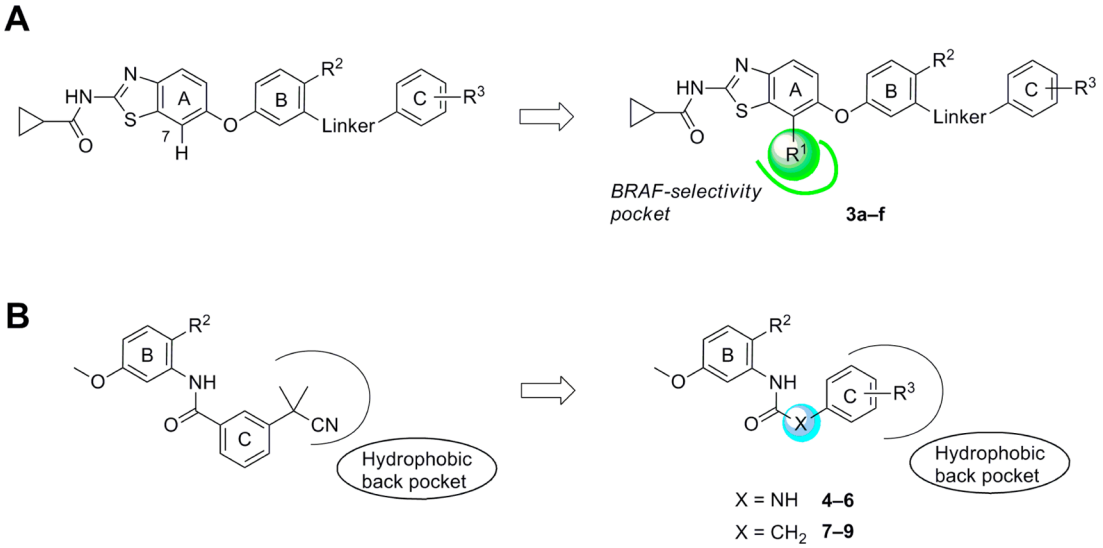

Figure 4. Design approaches employed for the ring A moiety and the ring B–linker–ring C moiety. (A) Ring A moiety: introduction of an R^1 group at the *C*-7 position for targeting a BRAF-selectivity pocket adjacent to Phe595. (B) Ring B–linker–ring C moiety targeting the hydrophobic back pocket of BRAF: ureide derivatives **4–6** (linker: NHCONH) and acetamide derivatives **7–9** (linker: $NHCOCH_2$).

Scheme 1. Synthetic Strategy for the Preparation of *C*-7-Substituted 1,3-Benzothiazole Intermediates 11 by the Regioselective Cyclization of Aniline 10

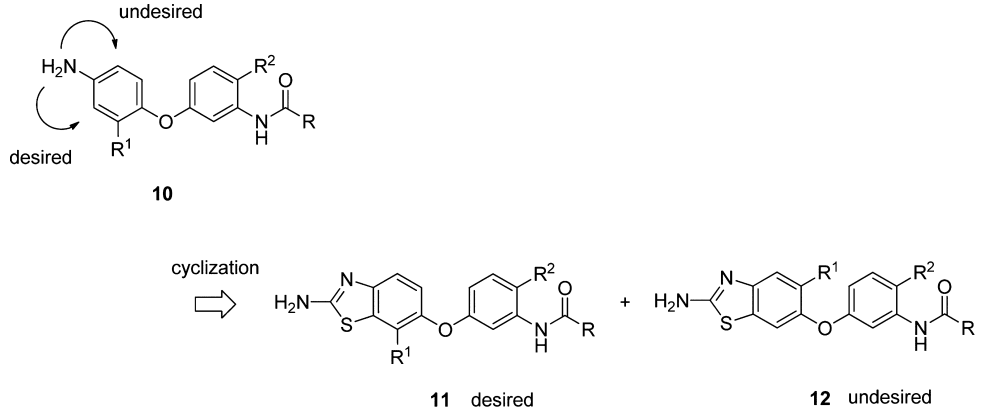

The *C*-7 unsubstituted (R^1 = H) 1,3-benzothiazole derivative **2** was synthesized by Kaufmann's method[19] from 4-phenoxylated aniline intermediate **10** (R^1 = H) using potassium thiocyanate (KSCN) and bromine (Br_2).[15] For the construction of the 1,3-benzothiazole scaffold, this methodology was frequently applied to symmetrical anilines such as *para*-substituted anilines[20] or *ortho*-substituted anilines such as 2-methoxy-4-substituted anilines.[21] In such cases, regioselectivity of the product formed was either not an issue or was controlled by the presence of an ortho substituent. In general, the electrophilic aromatic substitution occurs in a regioselective manner, and the regioselectivity is generally affected by substituents on the aromatic ring. Consequently, the regioselective cyclization of meta-substituted aniline **10** with a variety of R^1 substituents ($R^1 \neq H$) was of great interest in order to enable the efficient synthesis of desired *C*-7 isomer **11** (Scheme 1). However, to the best of our knowledge, only a few publications describing the preparation of *C*-7-substituted 1,3-benzothiazoles by cyclization directly from meta-substituted anilines have been reported (Supporting Information, Table S2).[22−24] Therefore, we initiated synthetic studies on this scaffold.

In this article, we describe the design, synthesis, and structure–activity relationships (SAR) of novel DFG-out type selective kinase inhibitors targeting pan-RAF inhibition. In addition, the characterization of our development candidate **8B** using surface plasmon resonance (SPR) spectroscopy and its application to human cancer cells harboring either mutant *BRAF* or mutant *NRAS* are also discussed.

Chemistry. The precursor anilines **10a–d** for 1,3-benzothiazole formation were prepared as shown in Scheme 2. S_NAr displacement of nitrobenzenes **14a–c** with known phenol derivative **13**[15] in the presence of potassium carbonate (K_2CO_3) in *N*,*N*-dimethylformamide (DMF) gave the phenoxylated compounds **15a–c** in 70–98% yield. Reduction of the nitro group for **15a,c** was carried out using reduced iron (Fe(0)) in the presence of calcium dichloride ($CaCl_2$) in 90% ethanol/water to avoid side reactions such as defluorination (**10a**) or nitrile reduction (**10c**) under hydrogenation conditions using palladium on activated carbon (Pd/C). As a result, the corresponding anilines **10a,c** were obtained in 82–99% yield. For compound **15b**, hydrogenation of the nitro group using Pd/C gave the corresponding aniline **10b** in 92% yield. In this reaction, 1-methylpyrrolidone (NMP) was used as

dx.doi.org/10.1021/jm400778d | J. Med. Chem. XXXX, XXX, XXX–XXX

Scheme 2[a]

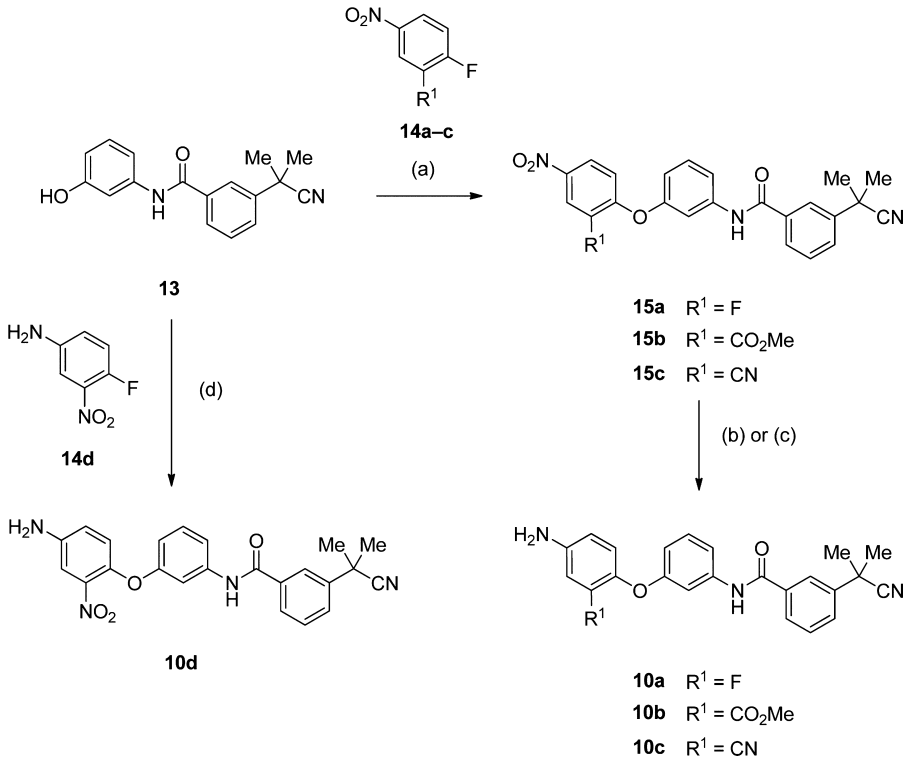

[a]Reagents and conditions: (a) K_2CO_3, DMF, 25–80 °C, 12–18 h (70–98%); (b) Fe(0), $CaCl_2$, EtOH/H_2O (9:1), 80–100 °C (82–99%); (c) H_2, 10% Pd/C, NMP/MeOH/THF (2:4:1), room temp., 14 h (92%); (d) Cs_2CO_3, DMF, 80 °C, 16 h (82%).

Table 1

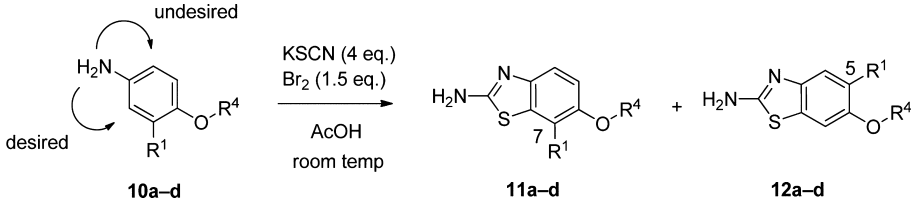

substrate[a]	R^1	yield[b] (%)			
		C-7 isomer **11**		*C*-5 isomer **12**	
10a	F	**11a**	N.D.[c]	**12a**	57
10b	CO_2Me	**11b**	90	**12b**	5
10c	CN	**11c**	81	**12c**	N.D.[c]
10d	NO_2	**11d**	73	**12d**	N.D.[c]

[a]R^4 means the 3-(1-cyano-1-methylethyl)benzamide moiety. [b]Isolated yield after conventional workup. Not optimized. [c]Not detected.

a cosolvent to dissolve substrate **15b**, which is insoluble in a mixed solvent of tetrahydrofuran (THF) and methanol (MeOH). The aniline derivative **10d** was directly synthesized from phenol **13** with 4-fluoro-3-nitroaniline **14d** (yield: 82%) using cesium carbonate (Cs_2CO_3) in DMF.

Next, the regioselective 1,3-benzothiazole formation reaction for anilines **10a–d** was investigated. We applied Kaufmann's conditions[19] to this reaction; the results are shown in Table 1. We first determined the optimal amounts of KSCN and Br_2 for this reaction. The optimized stoichiometry was 4 and 1.5 equivalents relative to the anilines **10a–d**, respectively. Lower amounts of KSCN or bromine caused low yields. The reaction of **10a** (R^1 = F) under these optimized conditions gave *C*-5 fluorinated isomer **12a** in 57% yield. In this experiment, the *C*-7 isomer **11a** was not isolated after conventional workup. Although the regioselectivity in **10a** was undesirable for our design concept, we continued our efforts to achieve the desired regioselectivity using other anilines **10b–d** possessing various R^1 substituents. Interestingly, the ring formation reactions of **10b** (R^1 = CO_2Me), **10c** (R^1 = CN), and **10d** (R^1 = NO_2) provided *C*-7 isomers **11b–d** with our desired regioselectivity in 73–90% isolated yields. Although the reaction of **10b** (R^1 = CO_2Me) provided the *C*-5 isomer in 5% yield, the reaction of **10c** (R^1 = CN) and **10d** (R^1 = NO_2) did not provide *C*-5 isomers. The change of regioselectivity between F and other R^1 groups such as NO_2 was also of great interest. This regioselectivity, *meta*-fluoroaniline provides a *C*-5 isomer[22] and *meta*-nitroaniline provides a *C*-7 isomer,[24] is consistent with other groups' reports (Supporting Information, Table S2). The ring formation reaction of thioureide derivatives using

dx.doi.org/10.1021/jm400778d | J. Med. Chem. XXXX, XXX, XXX–XXX

Scheme 3[a]

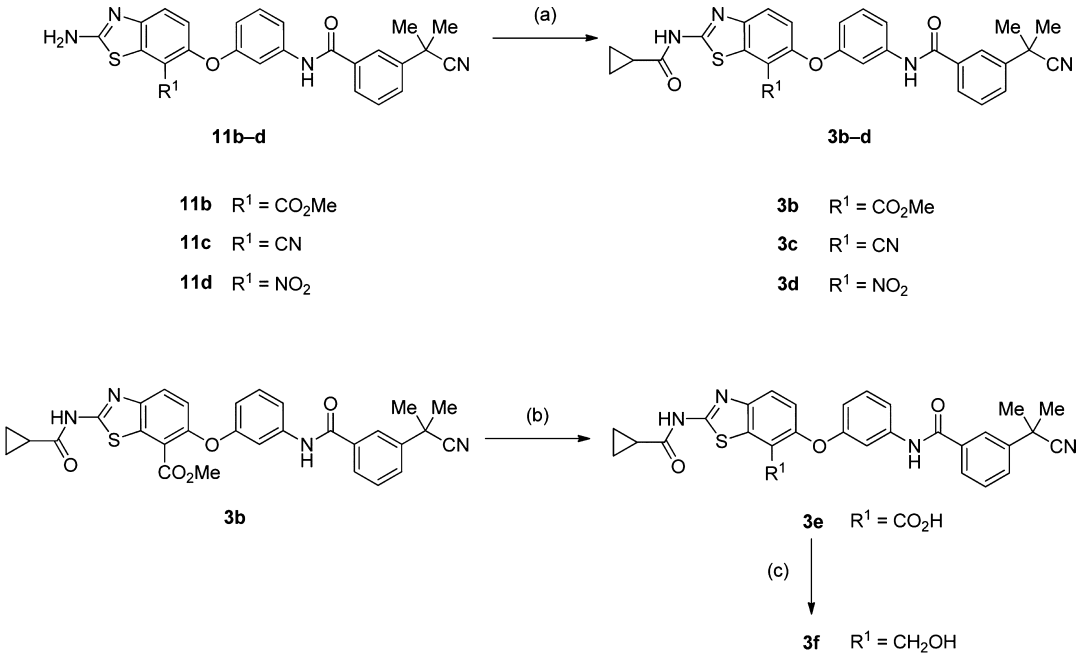

[a]Reagents and conditions: (a) cyclopropanecarbonyl chloride, pyridine, room temp., 2–4 h (68–79%); (b) $LiOH{\cdot}H_2O$, THF, MeOH, H_2O, room temp., 12 h (54%); (c) *iso*-butyl chloroformate, Et_3N, THF, 0°C, 0.5 h; then, $NaBH_4$, THF, MeOH, room temp., 2 h (55% in 2 steps).

bromine is also known as an alternative method to prepare the 1,3-benzothiazole ring. Some groups have reported that meta-substituted thioureides can provide *C*-5 or *C*-7 benzothiazoles in a regioselective manner (Supporting Information, Table S3).[25−28] Interestingly, the tendency for regioselectivity between both reactions is the same, and the direction of cyclization is determined by an R^1 substituent at the meta-position (F, *C*-5, CO_2Me; NO_2, *C*-7). Regarding the cyano group, our result is the first example that 7-cyano-1,3-benzothiazole can be prepared using the corresponding *meta*-cyanoaniline in a regioselective manner.

The synthesis of 1,3-benzothiazole derivatives **3b−f** is shown in Scheme 3. The acylation of 2-amino-1,3-benzothiazoles **11b−d** with cyclopropanecarbonyl chloride in pyridine gave the desired compounds **3b−d** in 68−79% yield. Hydrolysis of the methyl ester in **3b** with lithium hydroxide monohydrate ($LiOH{\cdot}H_2O$) gave the corresponding carboxylic acid **3e** in 54% yield. Reduction of the carboxyl group in **3e** was achieved via a mixed anhydride produced by the treatment of *iso*-butyl chloroformate with **3e** in the presence of triethylamine (Et_3N). The subsequent reduction of the obtained anhydride with sodium borohydride ($NaBH_4$) gave the desired hydroxymethyl derivative **3f** in 55% yield over 2 steps.

The synthesis of *C*-7 cyanated 1,3-benzothiazoles **4−9** possessing various ring B−linker−ring C moieties is shown in Scheme 4. This route was planned for optimization of the back pocket moiety. Therefore, we set the aniline derivatives **22A,B** as key intermediates for the synthesis of substituted phenyl ureides **4−6** and phenyl acetamides **7−9** in the last step in the route. The S_NAr displacement of 2-fluoro-5-nitrobenzonitrile **14c** with phenol **16A** in the presence of K_2CO_3 gave the phenoxylated aniline **17A** in 66% yield. Protection of the amine in **17A** by a trifluoroacetyl group was achieved in 67% yield using trifluoroacetic anhydride (TFAA), followed by reduction of the nitro group in **18A** under palladium-mediated hydrogenation conditions in a mixed solvent of NMP/MeOH to give the desired compound **19A** in 99% yield. The 1,3-benzothiazole formation reaction of **19A** using KSCN and bromine successfully provided the desired 7-cyano-2-amino-1,3-benzothiazole derivative **20A** in 81% yield. The acylation of **20A** with cyclopropanecarbonyl chloride (82% yield) and subsequent trifluoroacetyl cleavage from the resulting compound **21A** with $LiOH{\cdot}H_2O$ gave key intermediate **22A** in 95% yield.

The corresponding fluorinated key intermediate **22B** (R^2 = F) was prepared by a method similar to that used in the preparation of **22A** (R^2 = H). Reaction of **14c** with commercially available **16B** in the presence of K_2CO_3 followed by protection of the amino group using TFAA gave the desired compound **18B** in 93% in 2 steps. Reduction of the nitro group of **18B** by hydrogenation in the presence of Pd/C was carefully conducted, while monitoring the formation of defluorinated compound **19A**. Ultimately, this reaction gave the desired aniline **19B** in 99% yield without the contamination with **19A**. The 1,3-benzothiazole cyclization reaction of **19B** also successfully provided the desired isomer **20B** in 85% yield. The acylation of **20B** with cyclopropanecarbonyl chloride in the presence of pyridine in THF gave **21B** in comparatively lower yield (55%) than that for the preparation of **21A**. The reason for the reduced yield in this reaction is thought to result from cleavage of the trifluoroacetyl group in **20B**. Introduction of a fluorine atom at the ortho-position of anilide **20B** enhances the acidity of the trifluoroacetamide moiety, which may activate the nucleophilicity of the amide in its reaction with cyclopropanecarbonyl chloride to provide an asymmetrical imide at the anilino moiety (ring B). The postulated asymmetrical imide formed in situ should be easily cleaved under aqueous workup conditions to give the corresponding bis-cyclopropanecarbonylated compound as a significant byproduct. This contaminating byproduct, fortunately, could be removed by conventional silica gel column chromatography to give purified **21B**. Since the trifluoroacetamide of **21B** was highly resistant against the conventional alkaline hydrolysis conditions due to the presence

dx.doi.org/10.1021/jm400778d | *J. Med. Chem.* XXXX, XXX, XXX−XXX

Scheme 4[a]

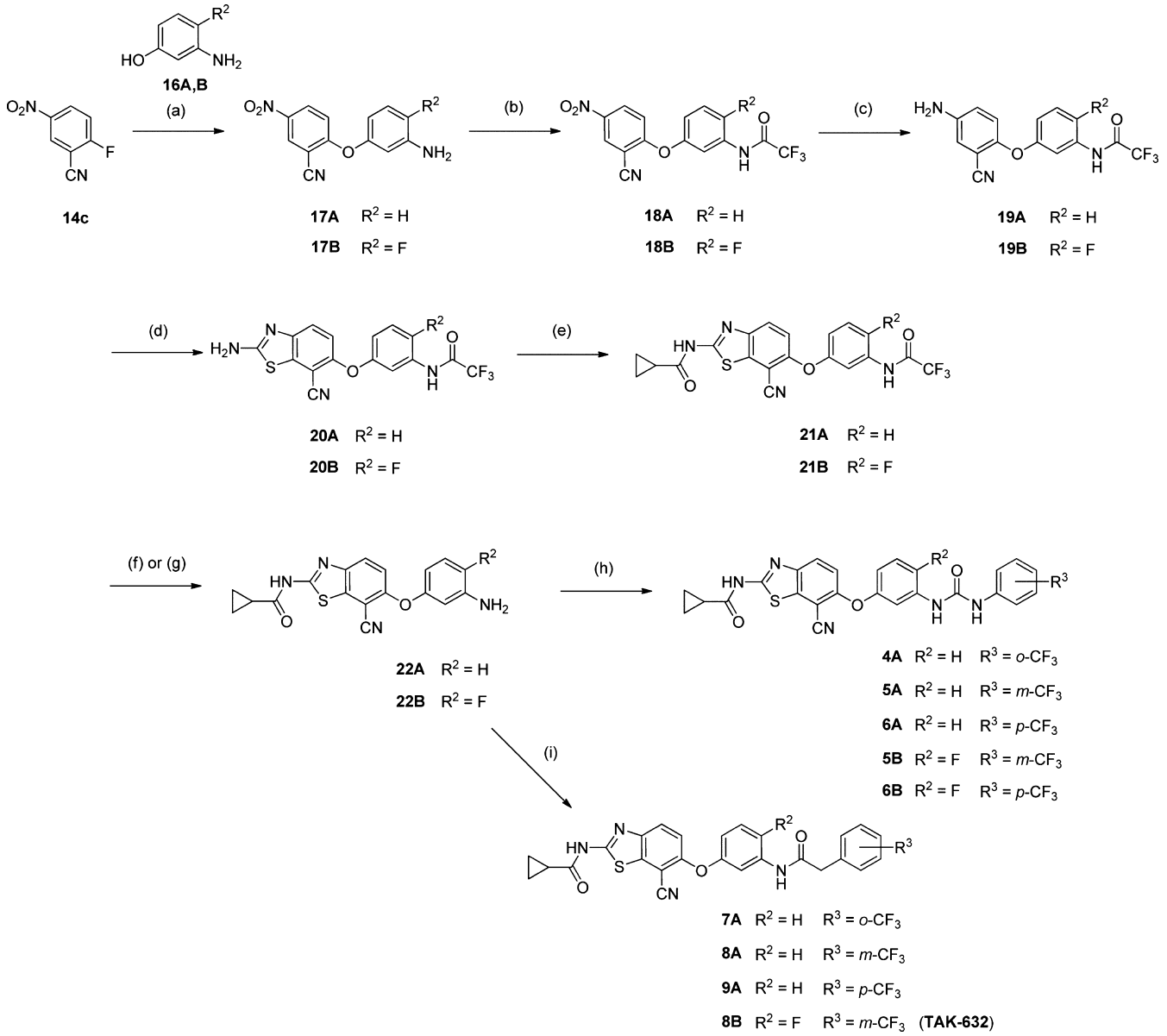

[a]Reagents and conditions: (a) **16A,B**, K_2CO_3, DMF, 25−60 °C, 2−4 h (66−100%); (b) TFAA, THF, room temp., 1−1.5 h (67−93%); (c) H_2, 10% Pd/C, MeOH, room temp., 2−8 h (99%); (d) KSCN, Br_2, AcOH, room temp., 12 h (81−85%); (e) cyclopropanecarbonyl chloride, pyridine, THF room temp., 6−16 h (55−82%); (f) LiOH·H_2O, THF/MeOH/H_2O (1:1:1), room temp., 18 h (95%); (g) $NaBH_4$, MeOH (2.4 v/v%), EtOH, room temp., 0.5 h (85%); (h) phenyl isocyanate, DMF, room temp., 12 h (28−94%); (i) phenyl acetic acid, HATU, pyridine, 85 °C, 4 h (57−74%).

of the *ortho*-fluorine group, hydride conditions using $NaBH_4$ were applied for cleavage of the trifluoroacetyl group. At first, deprotection using $NaBH_4$ was found to be very slow in EtOH. Optimal conditions were obtained by using 2−10 v/v% MeOH as an additive to accelerate the reaction. Use of greater than 10 v/v% of MeOH lowered yields due to undesirable hydrolysis of the cyclopropane carboxamide moiety at the 2-position. Ultimately, cleavage of the trifluoroacetyl group from **21B** using $NaBH_4$ in the presence of 2.4 v/v% MeOH in EtOH gave deprotected aniline **22B** in 85% yield.

Ureide formation from intermediate anilines **22A,B** with the corresponding isocyanate reagents was accomplished under conventional conditions to give the desired ureide derivatives **4A**, **5A,B**, and **6A,B** in 28−94% yield. Condensation of anilines **22A,B** with the corresponding phenyl acetic acids using hexafluorophosphate, *O*-(7-azabenzotriazol-1-yl)-*N*,*N*,*N*′,*N*′-tetramethyluronium (HATU), as a coupling reagent in the presence of pyridine provided the desired acetamide derivatives **7A**, **8A,B**, and **9A** in 57−74% yield.

RESULTS AND DISCUSSION

The 1,3-benzothiazoles **3b−f** that possess various R^1 substituents at the *C*-7 position were evaluated, and the SAR of **3b−f** compared to *C*-7 unsubstituted **2** (R^1 = H) is shown in Table 2. Nitro derivative **3b** (R^1 = NO_2) retained potent BRAF inhibition (IC_{50} = 25 nM), while demonstrating a 5-fold reduction in VEGFR2 inhibitory activity (IC_{50} = 70 nM) compared to that of compound **2**. The ratio of VEGFR2 IC_{50} to BRAF IC_{50} (V/B ratio) is a useful metric in discussing the selectivity of our BRAF inhibitors. Introduction of a nitro group

dx.doi.org/10.1021/jm400778d | J. Med. Chem. XXXX, XXX, XXX−XXX

Table 2. Structure–Activity Relationship for *C*-7-Substituted 1,3-Benzothiazoles (R^1)

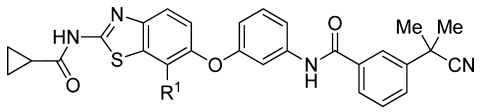

	R^1	kinase IC_{50} (nmol/L)[a] BRAF (V600E)	VEGFR2	ratio VEGFR2/BRAF (V600E)	cellular pMEK[b] IC_{50} (nmol/L)
2	H	25 (23–28)	14 (13–16)	0.56	240
3b	NO_2	25 (19–32)	70 (62–79)	2.8	29
3c	CN	13 (11–16)	76 (52–110)	5.8	34
3d	CO_2Me	12 (9.6–15)	33 (30–36)	2.8	24
3e	CO_2H	290 (160–500)	15 (13–17)	0.051	N.D.
3f	CH_2OH	24 (22–26)	7.4 (6.8–8.2)	0.31	170

[a] n = 2. 95% confidence intervals are shown in parentheses. [b] Cellular phosphorylation level of the downstream MEK (pMEK) was evaluated in HT-29 colon cancer cells (n = 1).

Table 3. Structure–Activity Relationship for Ureide Derivatives 4–6 Compared with that of Amide 3c

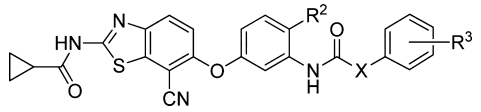

	X	R^2	R^3	kinase IC_{50} (nmol/L)[a] BRAF (V600E)	VEGFR2	ratio VEGFR2/BRAF (V600E)	cellular pMEK[b] IC_{50} (nmol/L)	PO AUC^c mice (μg h/kg)
3c	bond	H	*m*-$C(CH_3)_2CN$	13 (11–16)	76 (52–110)	5.8	34	0.149
4A	NH	H	*o*-CF_3	19 (16–23)	120 (82–170)	6.3	>500	0.058
5A	NH	H	*m*-CF_3	18 (5.6–58)	350 (310–410)	19	75	0.099
6A	NH	H	*p*-CF_3	18 (12–26)	330 (250–430)	18	110	0.431
5B	NH	F	*m*-CF_3	49 (17–140)	730 (650–810)	15	22	N.D.
6B	NH	F	*p*-CF_3	26 (13–51)	660 (530–830)	25	81	0.158

[a] n = 2. 95% confidence intervals are shown in parentheses. [b] Cellular phosphorylation level of the downstream MEK (pMEK) was evaluated in HT-29 colon cancer cells (n = 1). [c] Mean $AUC_{0-8\ h}$ values are shown (n = 2). Cassette dosing was of five compounds. Compounds (10 mg/kg) were administered in 0.5% methyl cellulose in distilled water.

Table 4. Structure–Activity Relationship for Acetamide Derivatives 7–9

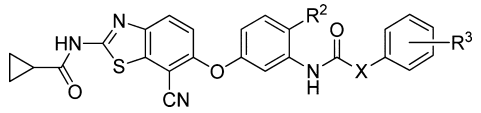

	X	R^2	R^3	kinase IC_{50} (nmol/L)[a] BRAF (V600E)	VEGFR2	ratio VEGFR2/BRAF (V600E)	cellular pMEK[b] IC_{50} (nmol/L)	PO AUC^c mice (μg h/kg)
7A	CH_2	H	*o*-CF_3	14 (9.2–20)	100 (89–110)	7.1	>500	0.255
8A	CH_2	H	*m*-CF_3	1.3 (0.68–2.6)	150 (130–190)	120	360	3.782
9A	CH_2	H	*p*-CF_3	9.5 (7.9–11)	190 (160–230)	20	320	0.123
8B	CH_2	F	*m*-CF_3	2.4 (0.45–12)	160 (140–180)	67	75	2.482

[a] n = 2. 95% confidence intervals are shown in parentheses. [b] Cellular phosphorylation level of the downstream MEK (pMEK) was evaluated in HT-29 colon cancer cells (n = 1). [c] Mean $AUC_{0-8\ h}$ values are shown (n = 2). Cassette dosing was of five compounds. Compounds (10 mg/kg) were administered in 0.5% methyl cellulose in distilled water.

at the *C*-7 position (**3b**) improved BRAF selectivity (V/B ratio for NO_2, 2.8; for H, 0.56). Furthermore, the cellular inhibitory activity of **3b** toward MEK phosphorylation (IC_{50} = 29 nM) was approximately 8-fold more potent than that for **2**.

Next, we evaluated the cyano derivative **3c** (R^1 = CN) and the methoxycarbonyl derivative **3d** (R^1 = CO_2Me). Compounds **3c** and **3d** showed a 2-fold increase in BRAF inhibitory potency (**3c**, 13 nM; **3d**, 12 nM) compared with that of the nitro derivative **3b**. The V/B ratio of **3c** is about 2-fold that of **3d** (V/B ratio for **3c**, 5.8; for **3d**, 2.8). The cellular pMEK inhibitory activity of compounds **3c,d** was equal to that of **3b** with an IC_{50} range of 24–34 nM. However, carboxylic acid derivative **3e** (R^1 = CO_2H) and hydroxymethyl derivative **3f** (R^1 = CH_2OH) showed different SAR. Compound **3e** showed reduced BRAF inhibitory activity (IC_{50} = 290 nM), whereas compound **3f** retained BRAF inhibition with an IC_{50} value of 24 nM but with reduced cellular pMEK inhibition (IC_{50} = 170 nM). In addition, the V/B ratios of **3e** and **3f** dropped to 0.051 and 0.31, respectively. As a result, we found the *C*-7 position to be significant in modulating the V/B ratio, and nitro (**3b**),

dx.doi.org/10.1021/jm400778d | J. Med. Chem. XXXX, XXX, XXX–XXX

cyano (**3c**), and methoxycarbonyl (**3d**) derivatives demonstrated high V/B ratios as well as potent cellular pMEK inhibition. The cyano derivative **3c** had the highest V/B ratio and was selected for further optimization.

In order to improve the V/B ratio further, we conducted chemical modification of the ring B−linker−ring C portion of **3c** to explore appropriate linkers (X) targeted for selective RAF inhibitors. First, we evaluated the ureide derivatives (X = NH, R^2 = H) possessing a trifluoromethyl group with various substitution positions such as *o*-CF_3 (**4A**), *m*-CF_3 (**5A**), and *p*-CF_3 (**6A**) (Table 3). Among them, the *m*-CF_3 (**5A**) and *p*-CF_3 (**6A**) derivatives showed improved V/B ratios (V/B ratio for *m*-, 19; for *p*-, 18) compared with that of the *o*-CF_3 derivative (V/B ratio for **4A**: 6.3). Thus, we selected *m*- and *p*-CF_3 groups on ring C and attempted to introduce a fluorine group at the metabolically labile site of ring B on the basis of our previous work.[15,17] Compound **5B** (R^2 = F, R^3 = *m*-CF_3) and **6B** (R^2 = F, R^3 = *p*-CF_3) showed comparable or slightly weaker BRAF inhibition (**5B** IC_{50}, 49 nM; **6B**, 26 nM) and V/B ratios similar to those of the corresponding unsubstituted (R^2 = H) derivatives **5A** or **6A**. Interestingly, the cellular pMEK inhibitory potency of these fluorinated compounds **5B** and **6B** increased, giving IC_{50} values of 22 and 81 nM, respectively. However, in spite of attractive cellular activity with improved BRAF selectivity, oral absorption for the ureide series was found to be extremely low with $AUC_{0-8\ h}$ values of 0.058−0.431 μg h/kg at a dose of 10 mg/kg in mice.

Next, we evaluated the acetamide derivatives (X = CH_2, R^2 = H) having a CF_3 group in three different positions as shown in Table 4. Meta-substitution of the CF_3 group (**8A**) showed notably enhanced BRAF inhibition, with potency at least 7-fold greater than that for the ortho (**7A**)- and para-substituted (**9A**) derivatives (IC_{50} values: *m*-, 1.3 nM; *p*-, 9.5 nM; *o*-, 14 nM). Reflecting the remarkable increase in BRAF inhibitory potency for **8A**, we observed that the V/B ratio increased to 120. These results encouraged us to synthesize fluorine derivative **8B** (R^2 = F). As we expected, compound **8B** showed a promising enzymatic profile for both BRAF inhibition (IC_{50}: 2.4 nM) and BRAF selectivity (V/B ratio: 67). In addition, this fluorinated derivative also exhibited potent cellular pMEK activity with an IC_{50} value of 75 nM. Furthermore, the pharmacokinetic (PK) evaluation of *m*-CF_3 derivatives **8A**,**B** showed significantly improved oral absorption with respective AUC values of 3.782 and 2.482 μg h/kg in mice, compared with those of the *o*- and *p*-CF_3 derivatives. On the basis of promising BRAF potency, selectivity, and good PK, compound **8B** was selected for further evaluation.

X-ray Cocrystal Structural Analysis of 8B with BRAF. We determined the X-ray cocrystal structure of **8B** bound to BRAF kinase (Figure 5).[29] The BRAF cocrystal structure (PDB code: 4KSP) revealed that the optimal compound **8B** is accommodated by the DFG-out conformation of BRAF, as we expected. Within the adenine site, the 1,3-benzothiazole-2-amide moiety forms two hydrogen bonds between the carbonyl of Cys532 and the NH of the 2-amide (3.0 Å), and between the NH of Cys532 and the *N*-3 nitrogen (3.4 Å). Since the measured distance between the carbonyl oxygen of the 2-amide and the *S*-1 sulfur (2.9 Å) is shorter than the sum of the corresponding van der Waals radii of the oxygen and sulfur atoms (3.32 Å),[30] the conformation of the 2-amide with respect to the 1,3-benzothiazole scaffold is held in a planar conformation by the sulfur−carbonyl interaction. These results for **8B** are consistent with those for **1** that we previously

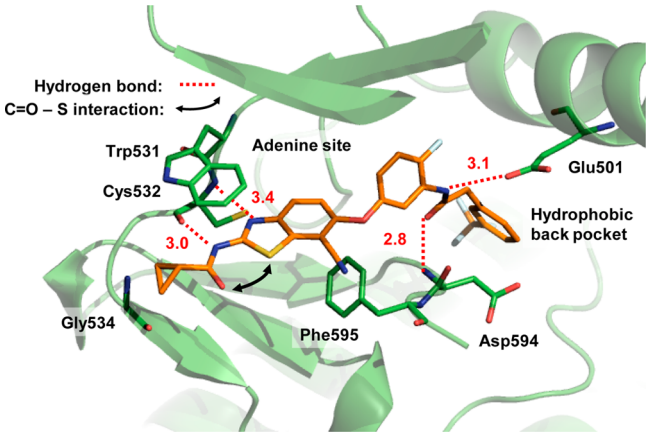

Figure 5. X-ray cocrystal structure of **8B** bound to BRAF (2.93 Å resolution).

reported.[15,18] Furthermore, it was also shown that the phenylacetamide linker of **8B** forms significant hydrogen bonds between the carboxylate of Glu501 and the NH of the acetamide (3.1 Å), and between the NH of Asp594 and the carbonyl of the acetamide (2.8 Å). The methylene of the phenylacetamide linker X in **8B** seems to be important for providing enough flexibility to fit into the back pocket of BRAF.

To clarify the importance of the phenylacetamide linker in **8B**, we also obtained an X-ray cocrystal structure of ureide **5B** (PDB code: 4KSQ).[31] The only difference between **8B** and **5B** is the linker X (**8B**, CH_2; **5B**, NH) (Figure 6). This single

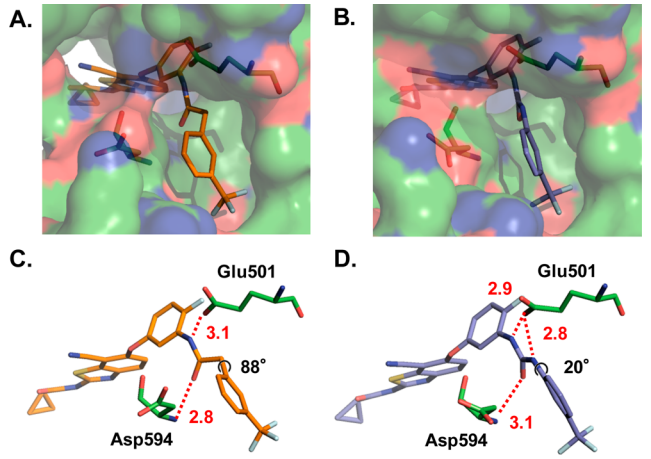

Figure 6. X-ray cocrystal structures of BRAF bound to acetamide derivative **8B** and of BRAF bound to the corresponding ureide derivative **5B**. (A) Trifluoromethyl-substituted benzene of **8B** in the back pocket region. (B) Trifluoromethyl-substituted benzene of the corresponding ureide **5B** in the back pocket region. (C) Binding mode of acetamide **8B** with Glu501 and Asp594 (2.93 Å resolution). (D) Binding mode of ureide **5B** with Glu501 and Asp594 (3.30 Å resolution).

change resulted in an approximately 20-fold increase in BRAF inhibitory activity for **8B** (IC_{50}: 2.4 nM) compared with that for **5B** (IC_{50}: 49 nM). The cocrystal structural analysis revealed that the *m*-CF_3-substituted benzene moieties of both **8B** and **5B** bind to the hydrophobic back pocket as we had envisioned (Figure 6A,B). In the cocrystal structure of **8B**, the phenylacetamide linker anchors the benzene moiety into a twisted orthogonal conformation with a dihedral angle of 88° at the

dx.doi.org/10.1021/jm400778d | J. Med. Chem. XXXX, XXX, XXX−XXX

CH_2 position (Figure 6C). However, the ureide **5B** shows a decreased dihedral angle of 20° at the corresponding NH position (Figure 6D). Since it is known that the acetamide linker provides more flexible conformations in a protein than the ureide moiety does,[32] the flexibility of phenylacetamide derivative **8B** allows optimal hydrophobic interaction between an 88° twisted *m*-CF_3-substituted benzene and a hydrophobic back pocket. We assume that this conformational change could account for the increase in RAF inhibition for **8B**.

Kinase Inhibitory Profiles of Compound 8B. The kinase inhibitory profile of compound **8B** against 26 different kinases is summarized in Table 5. Compound **8B** showed potent single-digit nanomolar inhibitory activity against BRAF(wt) and CRAF (BRAF(wt) IC_{50}, 8.3 nM; CRAF, 1.4 nM). In addition, compound **8B** inhibited Aurora B with an IC_{50} value of 66 nM. Another 8 out of 26 kinases, such as PDGFRβ, FGFR3, GSK3β, CDK2, P38α, PDGFRα, TIE2, and CDK1 were inhibited by **8B** with a range of IC_{50} values from 120−790 nM. CHK1, IKKβ, and MEK1 were inhibited over an IC_{50} range of 1400−1700 nM. No significant inhibition was observed against the other 12 kinases assayed. On the basis of these preclinical results, compound **8B** was found to be a selective kinase inhibitor targeting the RAF family kinases.

Table 5. Kinase Selectivity of Compound 8B

kinase	IC_{50} (nmol/L)[a]	kinase	IC_{50} (nmol/L)[a]
BRAF (wt)	8.3 (4.9−14)[b]	PKA	>10000
C-RAF	1.4 (0.75−2.6)[b]	PKCθ	>10000
FGFR3	280	CHK1	1400
PDGFRα	610	CK1δ	>10000
PDGFRβ	120	ERK1	>10000
EGFR	>10000	CDK1	790
Her2	>10000	CDK2	580
TIE2	740	Aurora B	66
c-Met	>10000	p38α	600
c-Kit	>10000	JNK1	>10000
Src	>10000	GSK3β	500
IR	>10000	MEK1	3700
IKKβ	3700	MEKK1	>10000

[a] n = 2. [b] 95% confidence intervals are in parentheses.

Dissociation Kinetics of Compound 8B Using Surface Plasmon Resonance Technology. To determine affinities and kinetic rate constants, compound **8B** was injected over immobilized BRAF(V600E) or CRAF, and surface plasmon resonance (SPR) was used to analyze the interaction (Biacore T100, http://www.biacore.com/). Compound **8B** showed similar equilibrium dissociation constants (K_D) against both BRAF and CRAF by SPR (BRAF K_D, 1.6×10^{-9}; CRAF, 0.52×10^{-9}; Table 6). The dissociation rate constant (k_{off}) and the residence time ($t_{1/2}$) of **8B** were 1.9×10^{-5} s^{-1} and 602 min for BRAF, 9.0×10^{-5} s^{-1} and 129 min for CRAF (Table 6). The dissociation parameters indicate that **8B** has slow dissociation kinetics (low k_{off}) along with long residence time binding to both BRAF and CRAF. In contrast, PLX4720,[33] a precursor analogue of vemurafenib (PLX4032), showed fast dissociation kinetics and short residence time under the same assay conditions (BRAF, k_{off} = 3.3×10^{-2} s^{-1}; $t_{1/2}$ = 21 s; CRAF, $k_{off\,(1)}$ = 2.2×10^{-3} s^{-1}; $t_{1/2\,(1)}$ = 5.3 min; $k_{off\,(2)}$ = 1.2×10^{-1} s^{-1}; $t_{1/2\,(2)}$ = 5.8 s). These results suggested that **8B** is a slow off-rate, pan-RAF inhibitor.

Table 6. Dissociation Kinetics of 8B Measured by SPR

	K_D[a]	apparent k_{off}[b] (sec^{-1})	dissociation half-life (min)
BRAF	1.6×10^{-9}	1.9×10^{-5}	602
CRAF:	5.2×10^{-10}	9.0×10^{-5}	129

[a] K_D: equilibrium dissociation constant, [b] K_{off}: dissociation rate constant.

Time Dependent Inhibition Properties of 8B against BRAF and CRAF. Some reported kinase inhibitors have been recognized as slow off-rate inhibitors with long residence times bound to the target protein.[34,35] These long residence times have been used to explain the potent drug properties found for these compounds.[36]

We evaluated the biochemical activity of **8B** against BRAF and CRAF at two different ATP concentrations of *K*m (low) and 1.0 mM (high, corresponding to 200-times the BRAF K_m and 2000-times the CRAF K_m) and two preincubation times (0 and 1 h) (Table 7). With 1 h of preincubation time, **8B** inhibited BRAF and CRAF in an ATP competitive manner (at low ATP concentrations BRAF IC_{50}: 15 nM; CRAF: 8.1 nM). The respective biochemical activity of **8B** against BRAF and CRAF reduced to IC_{50} values of 58 nM and 62 nM at high ATP concentrations.

Table 7. Biochemical Activities of 8B against BRAF(V600E) and CRAF with Differing Preincubation Times (0 or 1 h) and under Different ATP Concentrations: K_m (Low) or 1000 μM (High)

	kinase IC_{50} (nmol/L)[a]			
preincubation time:	0 h		1 h	
ATP concentration:	K_m[b]	1000 μM	K_m[b]	1000 μM
BRAF(V600E):	15	58	2.2	3.3
CRAF:	8.1	62	1.5	5.0

[a] n = 2. [b] K_m concentration of ATP; BRAF(V600E), [ATP] = 5 μM. CRAF: [ATP] = 0.5 μM.

Next, we examined the activity of **8B** with 1 h of preincubation time for the assay. At low ATP concentration, the inhibitory activity of **8B** increased in a time-dependent manner (BRAF IC_{50}, 2.2 nM; CRAF, 1.5 nM). At high ATP concentration, **8B** showed still potent inhibitory activity for both BRAF and CRAF (IC_{50}: 3.3 nM and 5.0 nM, respectively). These time-dependent inhibition properties with long residence times suggested that **8B** has the potential to demonstrate efficient inhibition of both BRAF and CRAF in cells.

In Vitro Pharmacology of Compound 8B. Reflecting the potent BRAF (V600E) inhibitory activity in vitro, compound **8B** inhibited phosphorylation of MEK (pMEK) in melanoma A375 cells ($BRAF^{V600E}$) with an IC_{50} value of 12 nM (Table 8). Downstream inhibition of ERK phosphorylation (pERK) was also observed in A375 cells with an IC_{50} value of 16 nM. Next, we also evaluated the cellular activity of **8B** against human melanoma HMVII cells ($NRAS^{Q61K}$/$BRAF^{G469V}$), which have been reported to be insensitive to selective BRAF(V600E) inhibitors such as vemurafenib.[14] In HMVII cells, signal transduction of the MAPK cascade is thought to be activated by mutated *NRAS* through the downstream BRAF(wt) and CRAF. However, continuous inhibition of BRAF or CRAF by the corresponding siRNA has been shown to induce downstream inhibition in cells with *RAS* mutation.[12] Interestingly,

dx.doi.org/10.1021/jm400778d | J. Med. Chem. XXXX, XXX, XXX−XXX

Table 8. Cellular Activities of pan-RAF Inhibitor 8B

	mutation status[a]		mean IC_{50} (nmol/L)[b]		
cell line	*BRAF*	*NRAS*	pMEK	pERK	proliferation GI_{50} (nmol/L)[c]
A375	V600E		12	16	66
HMVII	G469V	Q61K	49	50	200

[a]Mutational status determined from the Sanger Institute database. [b]Numbers represent average IC_{50} values derived from a Western blot assay after 2 h of **8B** administration. (n = 2). [c]Numbers represent average GI_{50} derived from a ATPlite cell proliferation assay after 72 h of **8B** administration. (n = 3).

8B demonstrated strong inhibition of pMEK and pERK in HMVII cells with IC_{50} values of 49 nM and 50 nM, respectively (Table 8). Furthermore, antiproliferative activity of **8B** was potent in both A375 and HMVII cells with GI_{50} values of 66 nM and 200 nM, respectively. On the basis of these preclinical results, compound **8B** was identified as an antitumor drug development candidate for patients with either $BRAF^{V600E}$ or *NRAS* mutation, based on its apparent suppression of RAF dimer feedback activation presumably caused by its slow off-rate and pan-RAF inhibitory profile.

Pharmacokinetic Profile and in Vivo Studies of Compound 8B in Rats. In a pharmacokinetic study, compound **8B** was administered using a solid dispersion (SD) formulation based on our previous research[15] because **8B** showed low solubility (<0.02 μg/mL) in pH 6.8 phosphate buffer.[37] An SD formulation of **8B** demonstrated dramatically improved solubility (740 μg/mL) in pH 6.8 phosphate buffer and exhibited significant oral absorption (at a dose of 25 mg/kg, AUC, 32.47 μg h/mL; *F*, 51.7%) in rats (Table 9). In a dog PK study, 10 mg/kg administration of the SD formulation of **8B** also showed superior oral bioavailability (*F*: 108%).

In vivo efficacy of **8B** was evaluated using an SD formulation in a human melanoma A375 ($BRAF^{V600E}$) xenograft model in F344 nude rats. Reflecting the potent in vitro pMEK inhibition, oral single administration of **8B** inhibited pERK in tumors at 8 h after its administration over a dose range of 1.9–24.1 mg/kg (Figure 7). In particular, 9.7–24.1 mg/kg dosing with **8B** strongly inhibited pERK levels to 11% of the control. We examined the antitumor efficacy of **8B** administered twice daily for 14 days in an A375 xenograft model in rats (Figure 8). Compound **8B** exhibited dose-dependent antitumor efficacy without severe body weight reduction over a dose range of 3.9–24.1 mg/kg. Significant tumor regression was observed at 9.7 mg/kg and 24.1 mg/kg (T/C = −2.1% and −12.1%, respectively).

Next, antitumor effects of **8B** in a human melanoma HMVII ($NRAS^{Q61K}/BRAF^{G469V}$) xenograft model were evaluated in rats (Figure 9). In this study, **8B** was orally administered as an SD formulation and suppressed the growth of HMVII tumors with

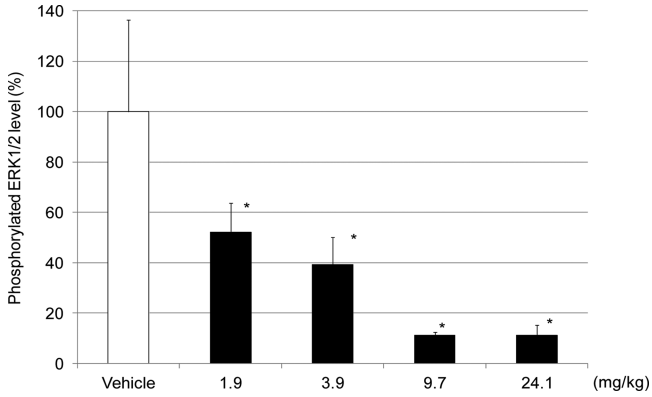

Figure 7. Mean (n = 3; *$P \leq 0.025$ compared with vehicle by the Shirley–Williams' test) phosphorylated ERK1/2 levels in the tumor in a human melanoma A375 ($BRAF^{V600E}$ mutant) xenograft model in rats, at 8 h after oral administration of **8B**. Data were detected by Western blotting. The solid dispersion formulation (**8B**/hydroxypropyl methylcellulose phthalate = 20:80) was delivered in distilled water.

T/C values of 52%, 26%, and 0% at doses of 3.9 mg/kg, 9.7 mg/kg, and 24.1 mg/kg, respectively. This antitumor efficacy was dose-dependent and significant ($p < 0.025$) compared with that of the vehicle control at all three doses. In this model, the HMVII tumor induced cancer cachexia and resulted in approximately 6% body weight loss in the vehicle control group over the 14-day administration period (body weight change: −8.6 g for the vehicle and +16.5 g for nontumor bearing). Interestingly, dose-dependent recovery of body weight loss was observed. In particular, the group at 24.1 mg/kg showed no signs of body weight loss (body weight change: +28.4 g). Recently, other DFG-out type (Type II) inhibitors were reported to have the potential to induce RAF dimerization and feedback activation in $BRAF^{wt}$ cells, similar to DFG-in type (Type I) inhibitors.[38] Some inhibitors are not able to inhibit activated MAPK signaling in $BRAF^{wt}$ normal cells at their projected efficacious doses and induce hyperplasia in animal models.[39] However, a study of our DFG-out type inhibitor **8B** using an A375 ($BRAF^{V600E}$) xenograft model indicated that administration of **8B** did not induce pERK activation in normal skin tissues ($BRAF^{wt}$) at projected efficacious doses but slightly inhibited pERK at higher doses of 25 and 50 mg/kg (Supporting Information, Figure S1). Further characterization of how **8B** inhibits the feedback activation in $BRAF^{wt}$ cells is of great interest. The results of detailed biological studies of our compounds will be reported in due course.

CONCLUSIONS

We designed and synthesized selective kinase inhibitors targeting pan-RAF kinase activity. On the basis of the X-ray

Table 9. Mean[a] Pharmacokinetic Parameters for Compound 8B

dose (mg/kg)	animal	route	CL_{total} (mL/h/kg)	V_{dss} (mL/kg)	MRT (h)	AUC_{0-24h} (μg h/mL)	% *F* (%)
1[b]	rat	iv	400 ± 29	1872 ± 71	4.69 ± 0.25	2.512 ± 0.18	
25[c]	rat	oral			6.27 ± 0.37	32.47 ± 4.68	51.7 ± 8.3
1[b]	dog	iv	704 ± 68	1568 ± 226	2.23 ± 0.27	1.429 ± 0.13	
10[c]	dog	oral			7.12 ± 0.76	15.48 ± 2.00	108 ± 8.0

[a]Values shown are the mean ± SD of data (n = 3). [b]Delivered in 1,3-butane-diol/DMA (1:1). [c]Delivered as a solid dispersion formulation (**8B**/hydroxypropyl methylcellulose phthalate = 20:80).

dx.doi.org/10.1021/jm400778d | J. Med. Chem. XXXX, XXX, XXX–XXX

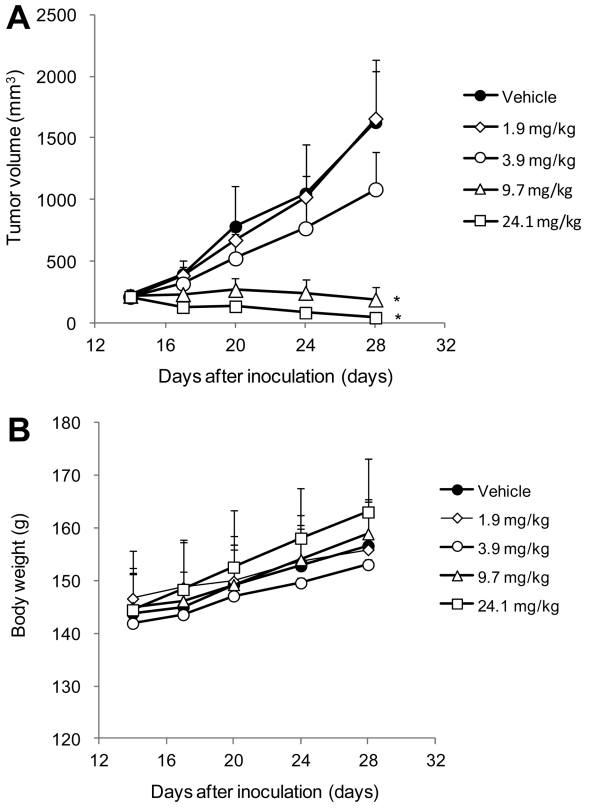

	Dose (mg/kg)	*T/C* (%)	Body weight change (g)
Vehicle	–	100	12.9
8B	1.9	103	9.3
8B	3.9	62.2	11.2
8B	9.7	−2.1	14.0
8B	24.1	−12.1	18.6

Figure 8. Antitumor activity of a solid dispersion of **8B** (p.o., b.i.d.) in human melanoma A375 ($BRAF^{V600E}$ mutant) bearing F344 nude rats (A) Mean ($n = 4$; $^*P \leq 0.025$ compared with the vehicle at day 14 by a one-tailed Shirley Williams' test) tumor volumes. (B) Mean ($n = 4$; $^*P \leq 0.025$ compared with the vehicle at day 14 by a one-tailed Shirley Williams' test) body weight change. The solid dispersion formulation (**8B**/hydroxypropyl methylcellulose phthalate =20:80) was delievered in distilled water.

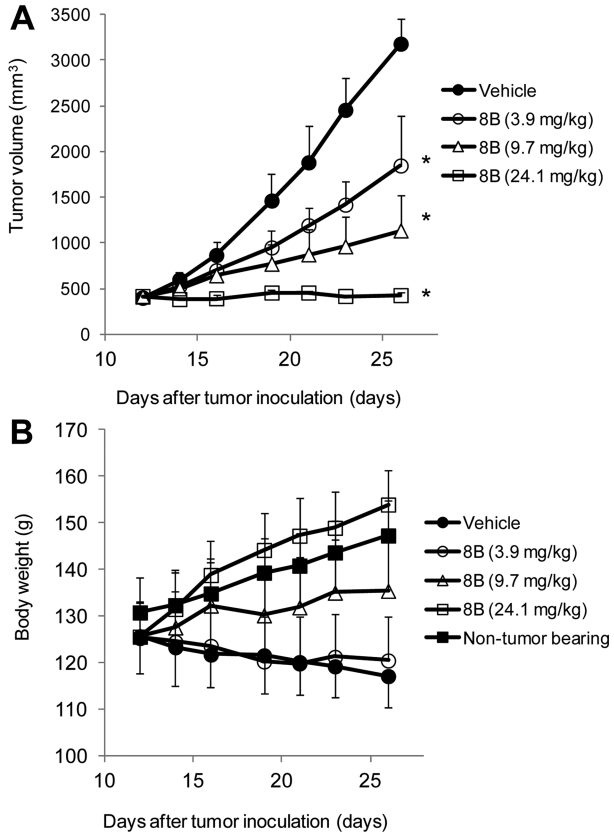

	Dose (mg/kg)	*T/C* (%)	Body weight change (g)
Non-tumor bearing	N/A	N/A	16.5
Vehicle	–	100	−8.6
8B	3.9	52	−4.8
8B	9.7	26	9.8
8B	24.1	0	28.4

Figure 9. Antitumor activity of a solid dispersion of **8B** in human melanoma HMVII ($NRAS^{Q61K}$/$BRAF^{G469V}$ mutant) bearing F344 nude rats (A) Mean ($n = 4$; $^*P \leq 0.025$ compared with the vehicle at day 14 by a one-tailed Shirley Williams' test) tumor volumes. (B) Mean ($n = 4$; $^*P \leq 0.025$ compared with the vehicle at day 14 by a one-tailed Shirley Williams' test) body weight change. The solid dispersion formulation (**8B**/hydroxypropyl methylcellulose phthalate = 20:80) was delievered in distilled water.

cocrystal structures of compound **1** with both BRAF (PDB code: 4DBN) and VEGFR2 (PDB code: 3VNT), *C*-7 substitution of lead compound **2** proved to be a fruitful approach to enhancing RAF inhibitory potency relative to VEGFR2. These novel compounds were efficiently prepared by the regioselective *C*-7-substituted 1,3-benzothiazole ring formation reaction of meta-substituted anilines with KSCN and bromine. Various substituents, such as NO_2, CN, and CO_2Me, provided good regioselectivity. Among these scaffolds, the 7-cyano derivatives showed enhanced BRAF selectivity over VEGFR2 as well as potent cellular pMEK inhibitory activity.

Subsequent optimization of the ring B−linker−ring C domain provided the *m*-CF_3-substituted phenylacetamide derivative **8B** as a potent pan-RAF inhibitor with favorable in vitro activity (BRAF(V600E) IC_{50}, 2.4 nM; BRAF(wt), 8.3 nM; CRAF, 1.4 nM; pMEK (A375) IC_{50}, 12 nM; pMEK (HMVII), 49 nM; V/B ratio, 67). In addition, compound **8B** was shown preclinically to be a selective kinase inhibitor targeting pan-RAF kinase activity by testing against a panel of kinases. X-ray cocrystal structure analysis revealed that **8B** occupies the ATP site of BRAF in the DFG-out conformation. Furthermore, the flexible acetamide linker provides a more twisted conformation for ring C that can interact more effectively with the hydrophobic back pocket than is observed for the ureide derivative (dihedral angles of 88° for the acetamide linker and 20° for the ureide linker).

An SPR study revealed that compound **8B** is a slow off-rate inhibitor of both BRAF and CRAF. Reflecting the slow off-rate property, compound **8B** demonstrated potent inhibitory activity even at high ATP concentration (BRAF(V600E) IC_{50}, 3.3 nM; CRAF, 5.0 nM) with 1 h of preincubation in a biochemical assay.

dx.doi.org/10.1021/jm400778d | *J. Med. Chem.* XXXX, XXX, XXX−XXX

In vitro pharmacological studies revealed that compound **8B** possesses significant cellular activity against *BRAF*^{V600E} and *NRAS* mutated cancer cell lines. In vivo pharmacological evaluation in a melanoma A375 (*BRAF*^{V600E}) xenograft model in rats revealed potent inhibition of the MAPK cascade in tumor cells after a single oral administration of **8B** at doses of 4−25 mg/kg. Furthermore, twice daily, 14 days of repetitive administration of **8B** demonstrated regressive antitumor efficacy at doses of 4−25 mg/kg without body weight changes. Moreover, compound **8B** induced regression in HMVII (*NRAS*^{Q61K}) tumors and restored body weight loss derived from HMVII tumor-induced cachexia.

These results suggested that slow off-rate pan-RAF inhibitors could represent a second generation of RAF inhibitors to be tested in the clinic for the treatment of human cancer harboring either *BRAF*^{V600E} or *NRAS* mutation. Along with another pan-RAF inhibitor MLN2480 under phase I clinical study by Takeda,[40] we selected compound **8B** (TAK-632) as an alternative development candidate.

EXPERIMENTAL SECTION

General Chemistry Information. The starting materials, reagents, and solvents for reactions were of reagent grade and were used as purchased. Thin-layer chromatography (TLC) was carried out using Merck Kieselgel 60, 63−200 mesh, F254 plates, or Fuji Silysia Chemical Ltd., 100−200 mesh, NH plates. Chromatographic purification was carried out using silica gel (Merck, 70−230 mesh) or basic silica gel (Fuji Silysia Chemical Ltd., DM1020, 100−200 mesh). Melting points were obtained using an OptiMelt melting point apparatus MPA100 and are uncorrected. Proton nuclear magnetic resonance ^{1}H NMR spectra were recorded using a Bruker AVANCE II (300 MHz) spectrometer with tetramethylsilane (TMS) as an internal standard. The NMR data are given as follows: chemical shift (δ) in ppm, multiplicity (where applicable), coupling constants (J) in Hz (where applicable), and integration (where applicable). Multiplicities are indicated by s (singlet), d (doublet), t (triplet), q (quartet), dd (doublet of doublets), dt, (doublet of triplets), ddd (doublet of doublet of doublets), br s (broad singlet), or m (multiplet). MS spectra were collected with a Waters LC-MS system (ZMD-1) and were used to confirm ≥95% purity of each compound. The column used was an L-column 2 ODS (3.0 × 50 mm I.D., CERI, Japan) with a temperature of 40 °C and a flow rate of 1.2 mL/min. Mobile phase A was 0.05% TFA in ultrapure water. Mobile phase B was 0.05% TFA in acetonitrile, which was increased linearly from 5% to 90% over 2 min and 90% over the next 1.5 min, after which the column was equilibrated to 5% for 0.5 min. Elemental analyses (Anal.) and high-resolution mass spectroscopy (HRMS) were carried out at Takeda Analytical Laboratories, Ltd. Yields were not optimized.

*Methyl 6-[3-({[3-(1-Cyano-1-methylethyl)phenyl]carbonyl}amino)phenoxy]-2-[(cyclopropylcarbonyl)amino]-1,3-benzothiazole-7-carboxylate (**3b**).* To a solution of methyl 2-amino-6-[3-({[3-(1-cyano-1-methylethyl)phenyl]carbonyl}amino)phenoxy]-1,3-benzothiazole-7-carboxylate **11b** (0.92 g, 1.88 mmol) in pyridine (5 mL) was added cyclopropanecarbonyl chloride (371 μL, 4.1 mmol), and the mixture was stirred at room temperature for 2 h. The reaction mixture was concentrated under reduced pressure. The obtained residue was diluted with EtOAc (100 mL), washed with water (100 mL) and brine (100 mL), successively, and dried over anhydrous Na_2SO_4. Insoluble material was filtered off, and the filtrate was concentrated under reduced pressure. The obtained residue was suspended in MeOH (10 mL), and Na_2CO_3 (250 mg) was added to the mixture. The mixture was stirred at room temperature for 4 h. The reaction mixture was diluted with EtOAc (100 mL), washed with water (100 mL) and brine (100 mL), successively, and dried over anhydrous Na_2SO_4. Insoluble material was filtered off, and the filtrate was concentrated under reduced pressure. The obtained residue was successively purified by basic silica gel column chromatography (40−100% EtOAc in *n*-hexane) and silica gel column chromatography (40−60% EtOAc in *n*-hexane), and the obtained solution was concentrated under reduced pressure. The residue was recrystallized from EtOAc/*n*-hexane to give **3b** (706 mg, 68%) as pale-yellow crystals; mp 143−145 °C. ^{1}H NMR (DMSO-d_6, 300 MHz): δ 0.98 (d, J = 4.2 Hz, 4H), 1.73 (s, 6H), 1.96−2.08 (m, 1H), 3.81 (s, 3H), 6.72−6.79 (m, 1H), 7.25 (d, J = 8.7 Hz, 1H), 7.31−7.42 (m, 2H), 7.49−7.63 (m, 2H), 7.69−7.77 (m, 1H), 7.88 (dt, J = 7.7, 1.3 Hz, 1H), 7.97 (t, J = 1.7 Hz, 1H), 8.01 (d, J = 8.7 Hz, 1H), 10.31 (s, 1H), 12.69 (br s, 1H). MS (ESI+) m/z 555.25 (M + H)$^+$. Anal. Calcd for $C_{30}H_{26}N_4O_5S{\cdot}0.4H_2O$: C, 64.13; H, 4.81; N, 9.97. Found: C, 64.17; H, 4.81; N, 9.84.

*N-[3-({7-Cyano-2-[(cyclopropylcarbonyl)amino]-1,3-benzothiazol-6-yl}oxy)phenyl]-3-(1-cyano-1-methylethyl)benzamide (**3c**).* To a solution of *N*-{3-[(2-amino-7-cyano-1,3-benzothiazol-6-yl)oxy]-phenyl}-3-(1-cyano-1-methylethyl)benzamide **11c** (150 mg, 0.33 mmol) in pyridine (2 mL) was added cyclopropanecarbonyl chloride (59 μL, 0.66 mmol), and the mixture was stirred at room temperature for 2 h. The reaction mixture was concentrated under reduced pressure. The residue was suspended in EtOAc (50 mL), washed with 5% aqueous $NaHCO_3$ solution (50 mL) and brine (50 mL), successively, and dried over anhydrous Na_2SO_4. Insoluble material was filtered off, and the filtrate was concentrated under reduced pressure. The obtained residue was purified by silica gel column chromatography (30−100% EtOAc in *n*-hexane), and the obtained solution was concentrated under reduced pressure. The residue was recrystallized from EtOAc to give **3c** (119 mg, 69%) as colorless crystals; mp 273−275 °C. ^{1}H NMR (DMSO-d_6, 300 MHz): δ 0.90−1.09 (m, 4H), 1.74 (s, 6H), 1.96−2.10 (m, 1H), 6.93 (dd, J = 2.1, 7.7 Hz, 1H), 7.20 (d, J = 8.9 Hz, 1H), 7.45 (t, J = 8.1 Hz, 1H), 7.54−7.68 (m, 3H), 7.70−7.81 (m, 1H), 7.91 (d, J = 7.9 Hz, 1H), 8.00 (t, J = 1.7 Hz, 1H), 8.05 (d, J = 8.9 Hz, 1H), 10.43 (s, 1H), 13.01 (br s, 1H). MS (ESI) m/z 522.25 (M + H)$^+$. Anal. Calcd for $C_{29}H_{23}N_5O_3S$: C, 66.78; H, 4.44; N, 13.43. Found: C, 66.57; H, 4.46; N, 13.40.

The following compounds (**3d**) were prepared from the corresponding 2-amino-1,3-benzothiazole derivatives (**11d**) with cyclopropanecarbonyl chloride by a method similar to that described for **3c**.

*3-(1-Cyano-1-methylethyl)-N-[3-({2-[(cyclopropylcarbonyl)-amino]-7-nitro-1,3-benzothiazol-6-yl}oxy)phenyl]benzamide (**3d**).* Yield 79%, yellow crystals (recrystallized from EtOAc/*n*-hexane), mp 223−225 °C. ^{1}H NMR (DMSO-d_6, 300 MHz): δ 0.95−1.05 (m, 4H), 1.73 (s, 6H), 1.98−2.09 (m, 1H), 6.81−6.92 (m, 1H), 7.33−7.47 (m, 2H), 7.49−7.65 (m, 3H), 7.71−7.78 (m, 1H), 7.90 (dt, J = 7.8, 1.2 Hz, 1H), 7.99 (t, J = 1.7 Hz, 1H), 8.15 (d, J = 8.7 Hz, 1H), 10.38 (s, 1H), 12.90 (br s, 1H). MS (ESI) m/z 542.25 (M + H)$^+$. Anal. Calcd for $C_{28}H_{23}N_5O_5S$: C, 62.10; H, 4.28; N, 12.93. Found: C, 61.83; H, 4.36; N, 12.70.

*6-[3-({[3-(1-Cyano-1-methylethyl)phenyl]carbonyl}amino)-phenoxy]-2-[(cyclopropylcarbonyl)amino]-1,3-benzothiazole-7-carboxylic Acid (**3e**).* To a solution of **3b** (570 mg, 1.02 mmol) in a mixed solvent of THF/MeOH/H_2O (3:1:1, 10 mL) was added LiOH·H_2O (150 mg, 3.66 mmol), and the mixture was stirred at room temperature for 12 h. The reaction mixture was neutralized with 1 N HCl, diluted with EtOAc/THF (1:1, 200 mL), and washed with water (100 mL). The organic layer was concentrated under reduced pressure. The obtained residue was purified by silica gel column chromatography (0−10% MeOH in EtOAc), and the obtained solution was concentrated under reduced pressure to give **3e** (300 mg, 54%) as a colorless amorphous solid. ^{1}H NMR (DMSO-d_6, 300 MHz): δ 0.90−1.01 (m, 4H), 1.72 (s, 6H), 1.94−2.09 (m, 1H), 6.70 (dd, J = 2.0, 8.0 Hz, 1H), 7.21 (d, J = 8.7 Hz, 1H), 7.27−7.36 (m, 2H), 7.47−7.61 (m, 2H), 7.68−7.77 (m, 1H), 7.87 (d, J = 7.7 Hz, 1H), 7.92−7.99 (m, 2H), 10.30 (s, 1H), 12.61 (s, 1H), 13.55 (br s, 1H). MS (ESI) m/z 541.25 (M + H)$^+$. Anal. Calcd for $C_{29}H_{24}N_4O_5S{\cdot}0.8H_2O$: C, 62.76; H, 4.65; N, 10.09. Found: C, 62.75; H, 4.58; N, 9.93.

*3-(1-Cyano-1-methylethyl)-N-[3-({2-[(cyclopropylcarbonyl)-amino]-7-(hydroxymethyl)-1,3-benzothiazol-6-yl}oxy)phenyl]-benzamide (**3f**).* To a solution of **3e** (200 mg, 0.369 mmol) in THF (8 mL) were added triethylamine (101 μL, 0.738 mmol) and *iso*-butyl chloroformate (96 μL, 0.738 mmol) at 4 °C, and the mixture was stirred at 4 °C for 30 min. Insoluble material was filtered off, and the

dx.doi.org/10.1021/jm400778d | J. Med. Chem. XXXX, XXX, XXX−XXX

filtrate was concentrated under reduced pressure. The obtained residue was dissolved in THF (2 mL), and to the mixture were added $NaBH_4$ (42 mg, 1.10 mmol) and MeOH (2 mL), and the mixture was stirred at room temperature for 2 h. The reaction mixture was concentrated under reduced pressure. The obtained residue was diluted with EtOAc (20 mL), washed with 1 N HCl (5 mL), 5% aqueous $NaHCO_3$ solution (10 mL) and brine (5 mL), successively, and dried over anhydrous Na_2SO_4. Insoluble material was filtered off, and the filtrate was concentrated under reduced pressure. The obtained residue was purified by silica gel column chromatography (20−60% EtOAc in *n*-hexane), and the obtained solution was concentrated under reduced pressure to give **3f** (108 mg, 55%) as pale yellow crystals; mp 152−153 °C. ^{1}H NMR (DMSO-d_6, 300 MHz) δ 0.90−1.00 (m, 4H), 1.73 (s, 6H), 1.93−2.07 (m, 1H), 4.74 (d, J = 5.1 Hz, 2H), 5.65 (t, J = 5.3 Hz, 1H), 6.66−6.77 (m, 1H), 7.09 (d, J = 8.5 Hz, 1H), 7.33 (t, J = 8.2 Hz, 1H), 7.37 (t, J = 2.2 Hz, 1H), 7.51 (dd, J = 0.9, 8.3 Hz, 1H), 7.57 (t, J = 7.8 Hz, 1H), 7.65 (d, J = 8.7 Hz, 1H), 7.69−7.79 (m, 1H), 7.83−7.92 (m, 1H), 7.97 (t, J = 1.8 Hz, 1H), 10.33 (s, 1H), 12.51 (br s, 1H). MS (ESI) m/z 527.20 $(M + H)^+$. Anal. Calcd for $C_{29}H_{26}N_4O_4S{\cdot}0.25H_2O$: C, 65.58; H, 5.03; N, 10.55. Found: C, 65.65; H, 5.16; N, 10.42.

*N-{7-Cyano-6-[3-({[2-(trifluoromethyl)phenyl]carbamoyl}amino)-phenoxy]-1,3-benzothiazol-2-yl}cyclopropanecarboxamide (**4A**).* To a solution of 1-isocyanato-2-(trifluoromethyl)benzene (63 μL, 0.44 mmol) in DMF (2 mL) was added *N*-[6-(3-aminophenoxy)-7-cyano-1,3-benzothiazol-2-yl]cyclopropanecarboxamide **22A** (120 mg, 0.34 mmol) at room temperature. The mixture was stirred at room temperature for 12 h and was diluted with EtOAc (10 mL). The mixture was washed with 5% aqueous $NaHCO_3$ (5 mL) and brine (5 mL), successively, dried over anhydrous Na_2SO_4, filtered, and evaporated. The resulting material was purified by basic silica gel column chromatography (60−100% EtOAc in *n*-hexane). Desired fractions were combined and evaporated in vacuo. The oily residue was crystallized from EtOAc (4 mL). The crystalline solid was collected by filtration using 50% EtOAc in *n*-hexane to give **4A** (107 mg, 58%) as colorless crystals; mp 181−183 °C. ^{1}H NMR (DMSO-d_6, 300 MHz): δ 0.89−1.07 (m, 4H), 1.93−2.13 (m, 1H), 6.64−6.90 (m, 1H), 7.10−7.23 (m, 2H), 7.24−7.33 (m, 1H), 7.32−7.43 (m, 2H), 7.62 (t, J = 7.6 Hz, 1H), 7.67 (d, J = 7.9 Hz, 1H), 7.88 (d, J = 8.1 Hz, 1H), 8.03 (d, J = 9.1 Hz, 1H), 8.10 (s, 1H), 9.53 (s, 1H), 13.00 (s, 1H). MS (ESI) m/z 538.2 $(M + H)^+$. Anal. Calcd for $C_{26}H_{18}F_3N_5O_3S{\cdot}0.5H_2O$: C, 57.14; H, 3.50; N, 12.81, Found: C, 57.43; H, 3.79; N, 12.42.

The following compounds (**5A**,**B** and **6A**,**B**) were prepared from the corresponding aniline derivatives (**22A**,**B**) with the corresponding isocyanate reagents by a method similar to that described for **4A**.

*N-{7-Cyano-6-[3-({[3-(trifluoromethyl)phenyl]carbamoyl}amino)-phenoxy]-1,3-benzothiazol-2-yl}cyclopropanecarboxamide (**5A**).* Yield 28%, colorless crystals (recrystallized from EtOAc/*n*-hexane), mp 269−270 °C. ^{1}H NMR (DMSO-d_6, 300 MHz): δ 0.83−1.12 (m, 4H), 1.91−2.16 (m, 1H), 6.77 (dd, J = 2.0, 8.0 Hz, 1H), 7.15 (d, J = 9.0 Hz, 1H), 7.20−7.44 (m, 4H), 7.44−7.66 (m, 2H), 7.96 (s, 1H), 8.03 (d, J = 9.0 Hz, 1H), 9.01 (s, 1H), 9.08 (s, 1H), 12.99 (s, 1H). HRMS (ESI) calcd for $C_{26}H_{18}F_3N_5O_3S$: 538.1155 $[M + H]^+$. Found: 538.1117.

*N-{7-Cyano-6-[4-fluoro-3-({[3-(trifluoromethyl)phenyl]-carbamoyl}amino)phenoxy]-1,3-benzothiazol-2-yl}-cyclopropanecarboxamide (**5B**).* Yield 85%, colorless crystals (recrystallized from EtOAc/*n*-hexane), mp 252−254 °C. ^{1}H NMR (DMSO-d_6, 300 MHz): δ 0.98 (d, J = 4.9 Hz, 4H), 2.00 (br s, 1H), 6.69−6.94 (m, 1H), 7.09 (d, J = 8.9 Hz, 1H), 7.22−7.43 (m, 2H), 7.52 (d, J = 5.1 Hz, 2H), 7.85−8.10 (m, 3H), 8.85 (s, 1H), 9.46 (s, 1H), 12.97 (br s, 1H). HRMS (ESI) calcd for $C_{26}H_{17}F_4N_5O_3S$: 556.1061 $[M + H]^+$. Found: 556.1049.

*N-{7-Cyano-6-[3-({[4-(trifluoromethyl)phenyl]carbamoyl}amino)-phenoxy]-1,3-benzothiazol-2-yl}cyclopropanecarboxamide (**6A**).* Yield 94%, colorless crystals (recrystallized from EtOAc), mp 217−218 °C. ^{1}H NMR (DMSO-d_6, 300 MHz): δ 0.93−1.08 (m, 4H), 1.99−2.07 (m, 1H), 6.74−6.85 (m, 1H), 7.17 (d, J = 9.0 Hz, 1H), 7.20−7.28 (m, 1H), 7.32−7.45 (m, 2H), 7.62 (s, 4H), 8.05 (d, J = 9.0 Hz, 1H), 9.01 (s, 1H), 9.13 (s, 1H), 13.00 (s, 1H). HRMS (ESI) calcd for $C_{26}H_{18}F_3N_5O_3S$ 538.1155 $[M + H]^+$. Found: 538.1107.

*N-{7-Cyano-6-[4-fluoro-3-({[4-(trifluoromethyl)phenyl]-carbamoyl}amino)phenoxy]-1,3-benzothiazol-2-yl}-cyclopropanecarboxamide (**6B**).* Yield 51%, colorless crystals (recrystallized from acetone/*n*-hexane), mp 176−177 °C. ^{1}H NMR (DMSO-d_6, 300 MHz): δ 0.84−1.22 (m, 4H), 1.86−2.07 (m, 1H), 6.68−6.92 (m, 1H), 7.13 (d, J = 8.9 Hz, 1H), 7.36 (dd, J = 9.1, 11.0 Hz, 1H), 7.55−7.73 (m, 4H), 7.91−8.13 (m, 2H), 8.87 (d, J = 2.5 Hz, 1H), 9.51 (s, 1H), 12.99 (s, 1H). MS (ESI) m/z 556.1 $(M + H)^+$. Anal. Calcd for $C_{26}H_{17}F_4N_5O_3S{\cdot}1.0H_2O$: C, 54.45; H, 3.34; N, 12.21. Found: C, 54.69; H, 3.23; N, 12.09.

*N-{7-Cyano-6-[3-({[2-(trifluoromethyl)phenyl]acetyl}amino)-phenoxy]-1,3-benzothiazol-2-yl}cyclopropanecarboxamide (**7A**).* To a solution of 2-(2-(trifluoromethyl)phenyl)acetic acid (138 mg, 0.68 mmol) in DMF (2 mL) was added **22A** (120 mg, 0.34 mmol) at room temperature. The mixture was stirred at room temperature for 12 h and was diluted with EtOAc (10 mL). The mixture was washed with aqueous 5% $NaHCO_3$ solution (5 mL) and brine (5 mL), successively, dried over anhydrous Na_2SO_4, filtered, and evaporated. The residue was purified by silica gel column chromatography (30−100% EtOAc in *n*-hexane). Desired fractions were combined and evaporated in vacuo. The crude material was crystallized from EtOAc to give **7A** (135 mg, 74%) as colorless crystals; mp 205−206 °C. ^{1}H NMR (DMSO-d_6, 300 MHz): δ 0.82−1.12 (m, 4H), 1.94−2.14 (m, 1H), 3.90 (s, 2H), 6.85 (td, J = 4.5, 2.5 Hz, 1H), 7.16 (d, J = 9.1 Hz, 1H), 7.28−7.57 (m, 5H), 7.57−7.78 (m, 2H), 8.02 (d, J = 8.9 Hz, 1H), 10.35 (s, 1H), 12.98 (br s, 1H). MS (ESI) m/z 537.2 $(M + H)^+$. Anal. Calcd for $C_{27}H_{19}F_3N_4O_3S$: C, 60.44; H, 3.57; N, 10.44. Found: C, 60.28; H, 3.63; N, 10.42.

The following compounds (**8A**,**B** and **9A**) were prepared from the corresponding aniline derivatives (**22A**,**B**) with the corresponding phenylacetic acids by a method similar to that described for **7A**.

*N-{7-Cyano-6-[3-({[3-(trifluoromethyl)phenyl]acetyl}amino)-phenoxy]-1,3-benzothiazol-2-yl}cyclopropanecarboxamide (**8A**).* Yield 57%, colorless crystals (recrystallized from EtOAc/n-heptane), mp 183−184 °C. ^{1}H NMR (DMSO-d_6, 300 MHz): δ 0.91−1.11 (m, 4H), 1.93−2.11 (m, 1H), 3.77 (s, 2H), 6.79−6.91 (m, 1H), 7.15 (d, J = 9.0 Hz, 1H), 7.31−7.43 (m, 2H), 7.43−7.48 (m, 1H), 7.50−7.65 (m, 3H), 7.67 (s, 1H), 8.02 (d, J = 9.0 Hz, 1H), 10.38 (s, 1H), 12.99 (s, 1H). MS (ESI) m/z 537.0 $(M + H)^+$. Anal. Calcd for $C_{27}H_{19}F_3N_4O_3S$: C, 60.44; H, 3.57; N, 10.44. Found: C, 60.28; H, 3.59; N, 10.42.

*N-{7-Cyano-6-[4-fluoro-3-({[3-(trifluoromethyl)phenyl]acetyl}-amino)phenoxy]-1,3-benzothiazol-2-yl}cyclopropanecarboxamide (**8B**).* Yield 60%, colorless crystals (recrystallized from EtOAc/*n*-heptane), mp 209−210 °C. ^{1}H NMR (DMSO-d_6, 300 MHz): δ 0.89−1.05 (m, 4H), 1.97−2.13 (m, 1H), 3.88 (s, 2H), 6.97 (dt, J = 8.7, 3.6 Hz, 1H), 7.08 (d, J = 9.0 Hz, 1H), 7.37 (dd, J = 9.1, 10.6 Hz, 1H), 7.49−7.64 (m, 3H), 7.68 (s, 1H), 7.83 (dd, J = 3.0, 6.4 Hz, 1H), 7.99 (d, J = 9.0 Hz, 1H), 10.21 (s, 1H), 12.97 (s, 1H). MS (ESI) m/z 555.50 $(M + H)^+$. Anal. Calcd for $C_{27}H_{18}F_4N_4O_3S$: C, 58.48; H, 3.27; N, 10.10. Found: C, 58.40; H, 3.18; N, 9.99.

*N-{7-Cyano-6-[3-({[4-(trifluoromethyl)phenyl]acetyl}amino)-phenoxy]-1,3-benzothiazol-2-yl}cyclopropanecarboxamide (**9A**).* Yield 69%, colorless crystals (recrystallized from EtOAc), mp 233−235 °C. ^{1}H NMR (DMSO-d_6, 300 MHz): δ 0.90−1.08 (m, 4H), 1.86−2.19 (m, 1H), 3.76 (s, 2H), 6.70−6.99 (m, 1H), 7.15 (d, J = 9.1 Hz, 1H), 7.30−7.41 (m, 2H), 7.45 (d, J = 1.7 Hz, 1H), 7.53 (d, J = 8.0 Hz, 2H), 7.68 (d, J = 8.0 Hz, 2H), 8.03 (d, J = 9.1 Hz, 1H), 10.39 (s, 1H), 13.00 (s, 1H). MS (ESI) m/z 537.2 $(M + H)^+$. Anal. Calcd for $C_{27}H_{19}F_3N_4O_3S$: C, 60.44; H, 3.57; N, 10.44, Found: C, 60.35; H, 3.81; N, 10.20.

*N-[3-(4-Amino-2-fluorophenoxy)phenyl]-3-(2-cyanopropan-2-yl)-benzamide (**10a**).* To a solution of 3-(2-cyanopropan-2-yl)-*N*-[3-(2-fluoro-4-nitrophenoxy)phenyl]benzamide **15a** (2.03 g, 4.83 mmol) in 90% EtOH in water were added Fe(0) (2.97 g, 53.1 mmol) and $CaCl_2$ (95%, 1.41 g, 12.1 mmol). The mixture was refluxed for 12 h, and was then cooled and filtered through a pad of Celite. The filtrate was concentrated under reduced pressure. The residue was partitioned between EtOAc (300 mL) and 5% aqueous $NaHCO_3$ solution (300 mL). The organic layer was washed with water (2 × 200 mL) and

dx.doi.org/10.1021/jm400778d | J. Med. Chem. XXXX, XXX, XXX−XXX

brine (200 mL), successively, dried over anhydrous Na_2SO_4, filtered, and evaporated. The residue was purified by silica gel column chromatography (30−100% EtOAc in *n*-hexane). Desired fractions were combined and evaporated to give **10a** (1.94 g, 99%) as yellow crystals; mp 77−78 °C. ^{1}H NMR (DMSO-d_6, 300 MHz): δ 1.74 (s, 6H), 5.34 (s, 2H), 6.35−6.44 (m, 1H), 6.49 (dd, J = 2.4, 13.2 Hz, 1H), 6.61−6.73 (m, 1H), 6.80−7.03 (m, 1H), 7.28 (t, J = 8.1 Hz, 1H), 7.36 (t, J = 2.1 Hz, 1H), 7.41−7.50 (m, 1H), 7.57 (t, J = 7.8 Hz, 1H), 7.67−7.79 (m, 1H), 7.83−7.94 (m, 1H), 7.99 (t, J = 1.8 Hz, 1H), 10.31 (s, 1H). MS (ESI) m/z 390.05 $(M + H)^+$.

*Methyl 5-amino-2-[3-({[3-(1-cyano-1-methylethyl)phenyl]carbonyl}amino)phenoxy]benzoate (**10b**).* To a solution of methyl 2-[3-({[3-(1-cyano-1-methylethyl)phenyl]carbonyl}amino)phenoxy]-5-nitrobenzoate **15b** (4.00 g, 8.70 mmol) in NMP/MeOH/THF (2:4:1) (70 mL) was added 10% Pd/C (400 mg), and the mixture was stirred at room temperature for 14 h under a hydrogen atmosphere (1 atm). Insoluble material was filtered off, and the filtrate was concentrated under reduced pressure. The obtained residue was diluted with EtOAc (200 mL), washed successively with water (2 × 100 mL) and brine (2 × 100 mL), and dried over anhydrous Na_2SO_4. Insoluble material was filtered off, and the filtrate was concentrated under reduced pressure. The obtained residue was purified by basic silica gel column chromatography (eluate: EtOAc), and the obtained solution was concentrated under reduced pressure to give **10b** (3.42 g, 92%) as a pale yellow oil. ^{1}H NMR (DMSO-d_6, 300 MHz): δ 1.74 (s, 6H), 2.69 (s, 3H), 5.33 (s, 2H), 6.44−6.63 (m, 1H), 6.71−6.96 (m, 2H), 7.07 (d, J = 2.6 Hz, 1H), 7.19−7.32 (m, 2H), 7.39−7.44 (m, 1H), 7.57 (t, J = 7.7 Hz, 1H), 7.68−7.80 (m, 1H), 7.83−7.94 (m, 1H), 7.98 (t, J = 1.7 Hz, 1H), 10.28 (s, 1H). MS (ESI) m/z 430.20 $(M + H)^+$.

The following compounds (**10c**) were prepared from the corresponding nitro derivatives (**15c**) using Fe(0) and $CaCl_2$ by a method similar to that described for **10a**.

*N-[3-(4-Amino-2-cyanophenoxy)phenyl]-3-(1-cyano-1-methylethyl)benzamide (**10c**).* Yield 82%, yellow oil. ^{1}H NMR (DMSO-d_6, 300 MHz): δ 1.74 (s, 6H), 5.48−5.66 (br s, 2H), 6.65−6.80 (m, 1H), 6.86−7.05 (m, 3H), 7.34 (t, J = 8.1 Hz, 1H), 7.42 (t, J = 2.1 Hz, 1H), 7.48−7.55 (m, 1H), 7.58 (t, J = 7.8 Hz, 1H), 7.69−7.81 (m, 1H), 7.84−7.94 (m, 1H), 8.00 (t, J = 1.7 Hz, 1H), 10.35 (s, 1H). MS (ESI) m/z 397.15 $(M + H)^+$.

*N-[3-(4-Amino-2-nitrophenoxy)phenyl]-3-(1-cyano-1-methylethyl)benzamide (**10d**).* To a mixture of 3-(1-cyano-1-methylethyl)-*N*-(3-hydroxyphenyl)benzamide **13** (20 g, 71.3 mmol) and 4-fluoro-3-nitroaniline **14d** (10.9 g, 69.9 mmol) in DMF (150 mL) was added Cs_2CO_3 (33.8 g, 104 mmol), and the mixture was stirred at 80 °C for 16 h. The reaction mixture was cooled to room temperature, and insoluble material was filtered off and washed with EtOAc. The filtrate and washings were combined, and the mixture was concentrated under reduced pressure. The obtained residue was diluted with EtOAc (300 mL), washed successively with water (300 mL) and brine (2 × 150 mL), and dried over anhydrous Na_2SO_4. Insoluble material was filtered off, and the filtrate was concentrated under reduced pressure. The obtained residue was purified by basic silica gel column chromatography (eluate: EtOAc), and the obtained solution was concentrated under reduced pressure. The residue was crystallized from EtOAc/*n*-hexane to give **10d** (23.8 g, 82%) as red-orange crystals; mp 137−138 °C. ^{1}H NMR (DMSO-d_6, 300 MHz): δ 1.74 (s, 6H), 5.71 (s, 2H), 6.61−6.74 (m, 1H), 6.93 (dd, J = 2.7, 8.7 Hz, 1H), 7.06 (d, J = 8.7 Hz, 1H), 7.20 (d, J = 2.7 Hz, 1H), 7.31 (t, J = 8.1 Hz, 1H), 7.39 (t, J = 2.1 Hz, 1H), 7.45−7.52 (m, 1H), 7.58 (t, J = 7.8 Hz, 1H), 7.68−7.79 (m, 1H), 7.90 (dt, J = 1.5, 7.8 Hz, 1H), 7.99 (t, J = 1.8 Hz, 1H), 10.33 (s, 1H). MS (ESI) m/z 417.15 $(M + H)^+$.

*Methyl 2-amino-6-[3-({[3-(1-cyano-1-methylethyl)phenyl]carbonyl}amino)phenoxy]-1,3-benzothiazole-7-carboxylate (**11b**).* Potassium thiocyanate (1.02 g, 10.5 mmol) was suspended in AcOH (10 mL), and the mixture was stirred at room temperature for 10 min. A solution of **10b** (1.13 g, 2.62 mmol) in AcOH (10 mL) was added to the obtained solution, and the mixture was further stirred at room temperature for 10 min. A solution of bromine (460 mg, 2.88 mmol) in AcOH (5 mL) was slowly added dropwise to the obtained solution, and the mixture was stirred at room temperature for 3 h. The resulting yellow insoluble material was filtered off and washed with AcOH. The filtrate and washings were combined, and the mixture was concentrated under reduced pressure. The obtained residue was suspended in EtOAc (200 mL), washed successively with saturated aqueous $NaHCO_3$ solution (100 mL) and brine (2 × 100 mL), and dried over anhydrous Na_2SO_4. Insoluble material was filtered off, and the filtrate was concentrated under reduced pressure. The residue was purified by basic silica gel column chromatography (40−100% EtOAc in *n*-hexane), and the obtained solution was concentrated under reduced pressure to give **11b** (1.15 g, 90%) as a colorless solid; mp 115−116 °C. ^{1}H NMR (DMSO-d_6, 300 MHz) δ 1.73 (s, 6H), 3.74 (s, 3H), 6.65−6.73 (m, 1H), 7.06 (d, J = 8.7 Hz, 1H), 7.25−7.38 (m, 2H), 7.44−7.63 (m, 5H), 7.67−7.77 (m, 1H), 7.82−7.91 (m, 1H), 7.97 (t, J = 1.7 Hz, 1H), 10.29 (s, 1H). HRMS (ESI) calcd for $C_{26}H_{22}N_4O_4S$: 487.1435 $[M + H]^+$. Found: 487.1406.

The following compounds (**11c,d** and **12a**) were prepared from the corresponding aniline derivatives (**10a,c,d**) using KSCN, Br_2, and AcOH by a method similar to that described for **11b**.

*N-{3-[(2-Amino-7-cyano-1,3-benzothiazol-6-yl)oxy]phenyl}-3-(1-cyano-1-methylethyl)benzamide (**11c**).* Yield 81%, yellow solid, mp 179−182 °C. ^{1}H NMR (DMSO-d_6, 300 MHz): δ 1.74 (s, 6H), 6.81−6.91 (m, 1H), 7.04 (d, J = 8.7 Hz, 1H), 7.41 (t, J = 8.1 Hz, 1H), 7.49−7.67 (m, 4H), 7.69−7.80 (m, 1H), 7.84−7.95 (m, 3H), 8.00 (t, J = 1.7 Hz, 1H), 10.39 (s, 1H). HRMS (ESI) calcd for $C_{25}H_{19}N_5O_2S$: 454.1332 $[M + H]^+$. Found: 454.1306.

*N-{3-[(2-Amino-7-nitro-1,3-benzothiazol-6-yl)oxy]phenyl}-3-(1-cyano-1-methylethyl)benzamide (**11d**).* Yield 73%, yellow solid; mp 202−204 °C. ^{1}H NMR (DMSO-d_6, 300 MHz): δ 1.73 (s, 6H), 6.71−6.88 (m, 1H), 7.21 (d, J = 8.7 Hz, 1H), 7.36 (t, J = 8.2 Hz, 1H), 7.44 (t, J = 2.1 Hz, 1H), 7.51−7.63 (m, 2H), 7.67−7.78 (m, 2H), 7.83−7.93 (m, 3H), 7.98 (t, J = 1.7 Hz, 1H), 10.34 (s, 1H). MS (ESI) m/z 474.20 $(M + H)^+$. Anal. Calcd for $C_{24}H_{19}N_5O_4S·0.2H_2O$: C, 60.42; H, 4.10; N, 14.68. Found: C, 60.48; H, 4.14; N, 14.49.

*N-{3-[(2-Amino-5-fluoro-1,3-benzothiazol-6-yl)oxy]phenyl}-3-(2-cyanopropan-2-yl)benzamide (**12a**).* Yield 57%, yellow crystals, mp 112−113 °C. ^{1}H NMR (DMSO-d_6, 300 MHz): δ 1.73 (s, 6H), 6.74 (dd, J = 2.0, 7.8 Hz, 1H), 7.25−7.37 (m, 2H), 7.40 (t, J = 2.0 Hz, 1H), 7.49−7.55 (m, 1H), 7.57 (t, J = 7.8 Hz, 1H), 7.61−7.69 (m, 3H), 7.70−7.78 (m, 1H), 7.85−7.92 (m, 1H), 7.98 (t, J = 1.6 Hz, 1H), 10.32 (s, 1H). HRMS (ESI) calcd for $C_{24}H_{19}FN_4O_2S$: 447.1286 $[M + H]^+$. Found: 447.1250.

*3-(1-Cyano-1-methylethyl)-N-[3-(2-fluoro-4-nitrophenoxy)phenyl]benzamide (**15a**).* To a mixture of **13** (2.0 g, 7.13 mmol) and 3,4-difluoronitrobenzene **14a** (1.19 g, 7.49 mmol) in DMF (15 mL) was added K_2CO_3 (1.48 g, 10.7 mmol) at room temperature. The mixture was stirred at 80 °C for 18 h, and the mixture was partitioned between EtOAc (200 mL) and water (200 mL). The organic layer was washed with water (200 mL) and brine (200 mL), successively, and dried over anhydrous Na_2SO_4. Insoluble material was filtered off, and the filtrate was concentrated under reduced pressure. The obtained residue was purified by silica gel column chromatography (EtOAc/*n*-hexane), and the obtained solution was concentrated under reduced pressure to give **15a** (2.09 g, 70%) as a yellow oil. ^{1}H NMR (DMSO-d_6, 300 MHz): δ 1.60−1.65 (m, 2H), 1.80−1.84 (m, 2H), 6.52 (dt, J = 6.6, 2.4 Hz, 1H), 7.09−7.14 (m, 2H), 7.32−7.33 (m, 1H), 7.54−7.56 (m, 2H), 7.80 (s, 1H), 7.84−7.88 (m, 1H), 9.43 (s, 1H), 10.16 (br s, 1H). MS (ESI) m/z 420.10 $(M + H)^+$.

The following compounds (**15b,c** and **17A,B**) were prepared from the 4-fluoronitrobenzene derivatives (**14b,c**) and the corresponding phenols (**13** and **16A,B**) using K_2CO_3 and DMF by a method similar to that described for **15a**.

*Methyl 2-[3-({[3-(1-Cyano-1-methylethyl)phenyl]carbonyl}amino)phenoxy]-5-nitrobenzoate (**15b**).* Yield 98%, colorless crystals, mp 144−145 °C. ^{1}H NMR (DMSO-d_6, 300 MHz): δ 1.75 (s, 6H), 3.88 (s, 3H), 6.90−6.99 (m, 1H), 7.14 (d, J = 9.3 Hz, 1H), 7.43−7.53 (m, 1H), 7.55−7.64 (m, 1H), 7.64−7.71 (m, 2H), 7.72−7.81 (m, 1H), 7.88−7.95 (m, 1H), 8.02 (t, J = 1.7 Hz, 1H), 8.41 (dd, J = 3.0, 9.3 Hz, 1H), 8.64 (d, J = 3.0 Hz, 1H), 10.49 (s, 1H). MS (ESI) m/z 460 $(M + H)^+$.

dx.doi.org/10.1021/jm400778d | J. Med. Chem. XXXX, XXX, XXX−XXX

*3-(1-Cyano-1-methylethyl)-N-[3-(2-cyano-4-nitrophenoxy)-phenyl]benzamide (**15c**).* Yield 94%, yellow oil. ^{1}H NMR (DMSO-d_6, 300 MHz): δ 1.75 (s, 6H), 7.01−7.19 (m, 2H), 7.55 (t, J = 8.1 Hz, 1H), 7.61 (t, J = 7.8 Hz, 1H), 7.68−7.80 (m, 2H), 7.81 (t, J = 2.1 Hz, 1H), 7.89−7.99 (m, 1H), 8.03 (t, J = 1.7 Hz, 1H), 8.48 (dd, J = 2.8, 9.4 Hz, 1H), 8.88 (d, J = 2.8 Hz, 1H), 10.56 (1H, s). MS (ESI) m/z 427 (M + H)$^+$.

*2-(3-Aminophenoxy)-5-nitrobenzonitrile (**17A**).* Yield 66%, yellow crystals (recrystallized from EtOAc/n-hexane), mp 131−133 °C. ^{1}H NMR (DMSO-d_6, 300 MHz): δ 5.48 (s, 2H), 6.31−6.37 (m, 1H), 6.38 (t, J = 2.2 Hz, 1H), 6.51−6.58 (m, 1H), 7.03 (d, J = 9.4 Hz, 1H), 7.11−7.20 (m, 1H), 8.45 (dd, J = 2.8, 9.4 Hz, 1H), 8.82 (d, J = 2.8 Hz, 1H). MS (ESI) m/z 255.95 (M + H)$^+$. Anal. Calcd for $C_{13}H_9N_3O_3$:C, 61.18; H, 3.55; N, 16.46. Found: C, 61.12; H, 3.46; N, 16.63.

*2-(3-Amino-4-fluorophenoxy)-5-nitrobenzonitrile (**17B**).* Yield 100%, beige crystals, mp 140−141 °C. ^{1}H NMR (DMSO-d_6, 300 MHz): δ 5.55 (s, 2H), 6.33−6.46 (m, 1H), 6.60 (dd, J = 3.0, 7.6 Hz, 1H), 7.02 (d, J = 9.4 Hz, 1H), 7.13 (dd, J = 8.7, 11.1 Hz, 1H), 8.44 (dd, J = 2.7, 9.4 Hz, 1H), 8.83 (d, J = 2.7 Hz, 1H). MS (ESI) m/z 273.95 (M + H)$^+$. Anal. Calcd for $C_{13}H_8FN_3O_3$: C, 57.15; H, 2.95; N, 15.38. Found: C, 57.22; H, 2.96; N, 15.34.

*N-[3-(2-Cyano-4-nitrophenoxy)phenyl]-2,2,2-trifluoroacetamide (**18A**).* To a solution of **17A** (18 g, 70.5 mmol) in THF (150 mL) was added trifluoroacetic anhydride (11.8 mL, 84.9 mmol) at 0 °C, and the mixture was stirred at room temperature for 1.5 h. The reaction mixture was diluted with EtOAc (500 mL), washed successively with water (150 mL), 5% aqueous $NaHCO_3$ solution (500 mL), and brine (500 mL), and dried over anhydrous Na_2SO_4. Insoluble material was filtered off, and the filtrate was concentrated under reduced pressure. The obtained residue was purified by silica gel column chromatography (10−40% EtOAc in n-hexane), and the obtained solution was concentrated under reduced pressure to give **18A** (16.6 g, 67%) as beige crystals; mp 190−191 °C. ^{1}H NMR (DMSO-d_6, 300 MHz) δ 7.09 (d, J = 9.3 Hz, 1H), 7.17−7.22 (m, 1H), 7.54−7.63 (m, 1H), 7.63−7.72 (m, 2H), 8.42−8.49 (m, 1H), 8.89 (d, J = 2.6 Hz, 1H), 11.46 (br s, 1H). MS (ESI) m/z 351 (M + H)$^+$. Anal. Calcd for $C_{15}H_8F_3N_3O_4$: C, 51.29; H, 2.30; N, 11.96. Found: C, 51.46; H, 2.33; N, 12.04.

The following compound (**18B**) was prepared from the aniline derivative (**17B**) using trifluoroacetic anhydride by a method similar to that described for **18A**.

*N-[5-(2-Cyano-4-nitrophenoxy)-2-fluorophenyl]-2,2,2-trifluoroacetamide (**18B**).* Yield 93%, colorless crystals, mp 168−169 °C. ^{1}H NMR (DMSO-d_6, 300 MHz): δ 7.06 (d, J = 9.4 Hz, 1H), 7.35−7.45 (m, 1H), 7.51−7.63 (m, 2H), 8.47 (dd, J = 2.8, 9.4 Hz, 1H), 8.88 (d, J = 2.8 Hz, 1H), 11.51 (s, 1H). Anal. Calcd for $C_{15}H_7F_4N_3O_4$: C, 48.79; H, 1.91; N, 11.38. Found: C, 48.85; H, 2.02; N, 11.30.

The following compounds (**19A,B**) was prepared from the nitro derivatives (**18A,B**) using H_2 and 10% Pd/C by a method similar to that described for **10b**.

*N-[3-(4-Amino-2-cyanophenoxy)phenyl]-2,2,2-trifluoroacetamide (**19A**).* Yield 99%, pale yellow oil. ^{1}H NMR (DMSO-d_6, 300 MHz): δ 5.55 (s, 2H), 6.81 (d, J = 8.1 Hz, 1H), 6.88−6.94 (m, 2H), 6.96−7.03 (m, 1H), 7.22 (t, J = 2.1 Hz, 1H), 7.32−7.42 (m, 1H), 7.41−7.50 (m, 1H), 11.28 (br s, 1H). MS (ESI) m/z 321.95 (M + H)$^+$. Anal. Calcd for $C_{15}H_{10}F_3N_3O_2$: C, 56.08; H, 3.14; N, 13.08. Found: C, 56.28; H, 3.17; N, 13.13.

*N-[5-(4-Amino-2-cyanophenoxy)-2-fluorophenyl]-2,2,2-trifluoroacetamide (**19B**).* Yield 99%, gray crystals, mp 136−137 °C. ^{1}H NMR (DMSO-d_6, 300 MHz): δ 5.53 (s, 2H), 6.84−7.00 (m, 4H), 7.09 (dd, J = 3.2, 6.2 Hz, 1H), 7.33 (t, J = 9.5 Hz, 1H), 11.20 (br s, 1H). MS (ESI) m/z 340.00 (M + H)$^+$. Anal. Calcd for $C_{15}H_9F_4N_3O_2$: C, 53.11; H, 2.67; N, 12.39. Found: C, 52.92; H, 2.80; N, 12.13.

The following compounds (**20A,B**) were prepared from the corresponding aniline derivatives (**19A,B**) using KSCN, Br_2, and AcOH by a method similar to that described for **11b**.

*N-{3-[(2-Amino-7-cyano-1,3-benzothiazol-6-yl)oxy]phenyl}-2,2,2-trifluoroacetamide (**20A**).* Yield 81%, yellow crystals, mp 263−264 °C. ^{1}H NMR (DMSO-d_6, 300 MHz): δ 6.89−7.00 (m, 1H), 7.06 (d, J = 8.9 Hz, 1H), 7.35 (t, J = 2.1 Hz, 1H), 7.44 (t, J = 8.1 Hz, 1H), 7.51−7.59 (m, 1H), 7.63 (d, J = 8.9 Hz, 1H), 7.92 (s, 2H), 11.30 (s, 1H). MS (ESI) m/z 379 (M + H)$^+$. Anal. Calcd for $C_{16}H_9F_3N_4O_2S{\cdot}0.5H_2O$: C, 49.61; H, 2.60; N, 14.46. Found: C, 49.65; H, 2.86; N, 14.30.

*N-{5-[(2-Amino-7-cyano-1,3-benzothiazol-6-yl)oxy]-2-fluorophenyl}-2,2,2-trifluoroacetamide (**20B**).* Yield 85%, pale yellow crystals, mp 251−253 °C. ^{1}H NMR (DMSO-d_6, 300 MHz): δ 7.00 (d, J = 8.9 Hz, 1H), 7.10−7.19 (m, 1H), 7.26 (dd, J = 3.1, 6.1 Hz, 1H), 7.42 (t, J = 9.5 Hz, 1H), 7.62 (d, J = 8.9 Hz, 1H), 7.91 (s, 2H), 11.34 (s, 1H). MS (ESI) m/z 397 (M + H)$^+$. Anal. Calcd for $C_{16}H_8F_4N_4O_2S$: C, 48.49; H, 2.03; N, 14.14. Found: C, 48.26; H, 2.26; N, 13.78.

The following compounds (**21A,B**) were prepared from the corresponding 2-amino-1,3-benzothiazole derivatives (**20A,B**) with cyclopropanecarbonyl chloride by a method similar to that described for **3c**.

*N-(7-Cyano-6-{3-[(trifluoroacetyl)amino]phenoxy}-1,3-benzothiazol-2-yl)cyclopropanecarboxamide (**21A**).* Yield 82%, colorless crystals (recrystallized from EtOAc), mp 243−244 °C. ^{1}H NMR (DMSO-d_6, 300 MHz): δ 0.80−1.13 (m, 4H), 1.92−2.11 (m, 1H), 6.93−7.15 (m, 1H), 7.22 (d, J = 8.9 Hz, 1H), 7.35−7.73 (m, 3H), 8.06 (d, J = 9.0 Hz, 1H), 11.0−12.1 (br s, 1H), 12.2−13.4 (br s, 1H). MS (ESI) m/z 446.95 (M + H)$^+$.

*N-(7-Cyano-6-{4-fluoro-3-[(trifluoroacetyl)amino]phenoxy}-1,3-benzothiazol-2-yl)cyclopropanecarboxamide (**21B**).* Yield 55%, colorless crystals (recrystallized from EtOAc/n-hexane), mp 242−243 °C. ^{1}H NMR (DMSO-d_6, 300 MHz): δ 0.95−1.05 (m, 4H), 1.97−2.09 (m, 1H), 7.16 (d, J = 9.0 Hz, 1H), 7.19−7.28 (m, 1H), 7.36 (dd, J = 3.0, 6.2 Hz, 1H), 7.46 (t, J = 9.5 Hz, 1H), 8.05 (d, J = 9.0 Hz, 1H), 11.36 (s, 1H), 12.99 (s, 1H). MS (ESI) m/z 465.1 (M + H)$^+$. Anal. Calcd for $C_{20}H_{12}F_4N_4O_3S$: C, 51.73; H, 2.60; N, 12.06. Found: C, 52.11; H, 2.85; N, 12.08.

*N-[6-(3-Aminophenoxy)-7-cyano-1,3-benzothiazol-2-yl]-cyclopropanecarboxamide (**22A**).* Compound **21A** (1.06 g, 2.37 mmol) was dissolved in a mixed solvent of THF/MeOH/H_2O (1:1:1) (75 mL), LiOH·H_2O (1.05 g, 25.7 mmol) was added, and the mixture was stirred at room temperature for 18 h. The reaction mixture was neutralized with 1 N HCl and concentrated under reduced pressure. The obtained precipitates were repeatedly washed with water to give **22A** (0.79 g, 95%) as colorless crystals; mp 233−234 °C. ^{1}H NMR (DMSO-d_6, 300 MHz): δ 0.90−1.14 (m, 4H), 1.96−2.11 (m, 1H), 5.33 (s, 2H), 6.18−6.30 (m, 2H), 6.37−6.49 (m, 1H), 6.98−7.07 (m, 1H), 7.10 (d, J = 9.1 Hz, 1H), 8.00 (d, J = 9.1 Hz, 1H), 12.96 (br s, 1H). MS (ESI) m/z 351.05 (M + H)$^+$. Anal. Calcd for $C_{18}H_{14}N_4O_2S{\cdot}0.5H_2O$: C, 60.15; H, 4.21; N, 15.59. Found: C, 60.31; H, 4.19; N, 15.57.

*N-[6-(3-Amino-4-fluorophenoxy)-7-cyano-1,3-benzothiazol-2-yl]-cyclopropanecarboxamide (**22B**).* To a solution of $NaBH_4$ (1.46 g, 38.6 mmol) in EtOH (20 mL) was added MeOH (0.5 mL). To this suspension was added **21B** (900 mg, 1.93 mmol) at 0 °C. The reaction mixture was stirred at 0 °C for 0.5 h then at room temperature for 0.5 h. The mixture was diluted with EtOAc (20 mL), and the resulting mixture was concentrated in vacuo. The resulting residue was diluted with EtOAc (200 mL), washed successively with 5% aqueous $NaHCO_3$ solution (100 mL) and brine (2 × 100 mL), and dried over anhydrous Na_2SO_4. Insoluble material was filtered off, and the filtrate was concentrated under reduced pressure. The obtained residue was purified by basic silica gel column chromatography (eluent: EtOAc), and the obtained solution was concentrated under reduced pressure. The residue was recrystallized from EtOAc/n-hexane to give **22B** (611 mg, 85%) as colorless crystals; mp 196−197 °C. ^{1}H NMR (DMSO-d_6, 300 MHz): δ 0.89−1.07 (m, 4H), 1.95−2.08 (m, 1H), 5.40 (s, 2H), 6.16−6.35 (m, 1H), 6.49 (dd, J = 3.0, 7.6 Hz, 1H), 6.96−7.11 (m, 2H), 8.00 (d, J = 8.9 Hz, 1H), 12.94 (br s, 1H). MS (ESI) m/z 369.1 (M + H)$^+$. Anal. Calcd for $C_{18}H_{13}FN_4O_2S$: C, 58.69; H, 3.56; N, 15.21. Found: C, 58.63; H, 3.58; N, 15.00.

■ ASSOCIATED CONTENT

Ⓢ Supporting Information

Information related to the feedback activation in fibroblast CsFb cells, reported regioselective/nonselective C-7 substituted 1,3-benzothiazole ring formation reaction of meta-substituted

dx.doi.org/10.1021/jm400778d | J. Med. Chem. XXXX, XXX, XXX−XXX

anilines and regioselective cyclization of meta-substituted thioureides, and assay protocols used in kinase enzyme assays, cellular assays, SPR assay, in vivo studies, solubility study, pharmacokinetic studies, and structural biology studies. This material is available free of charge via the Internet at http://pubs.acs.org.

Accession Codes

PDB accession codes are 4KSP for BRAF with **8B** and 4KSQ for BRAF with **5B**.

AUTHOR INFORMATION

Corresponding Authors

*(M.O.) Phone: +81-466-32-1158. Fax: +81-466-29-4448. E-mail: masanori.okaniwa@takeda.com.

*(M.H.) Phone: +81-466-32-1029. Fax: +81-466-29-4448. E-mail: masaaki.hirose@takeda.com.

*(T.I.) Phone: +81-466-32-1155. Fax: +81-466-29-4449. E-mail: tomoyasu.ishikawa@takeda.com.

Present Address

‖K.A.: Dart Neuroscience, 10420 Wateridge Circle, San Diego, CA 92121.

Notes

The authors declare no competing financial interest.

ACKNOWLEDGMENTS

We thank Tohru Miyazaki, and Takashi Imada for their support in the synthesis reactions. We express our gratitude to Yuka Hasegawa, Akiko Nakayama, Kazuyo Kakoi, and Katherine Galvin for their helpful support in biological evaluation. We thank Koji Mori, Shuuhei Yao, Hiroshi Miki, Taeko Yoshida, and Hidehisa Iwata for their assistance in evaluating the kinase inhibitory activities. We thank Yuuki Koudono for his assistance in preparing the SD formulation. We thank Douglas R. Cary for his helpful support in proofreading.

ABBREVIATIONS USED

^{1}H NMR, proton nuclear magnetic resonance; AUC, area under the blood concentration−time curve; CL_{total}, clearance; DMA, *N*,*N*-dimethylacetamide; ERK, extracellular signal-regulated kinase; ESI, electrospray ionization; HPLC, high-performance liquid chromatography; HRMS, high-resolution mass spectroscopy; K_D, equilibrium dissociation constants; k_{off}, dissociation rate constant; MAPK, mitogen-activated protein kinase; MEK, mitogen-activated protein kinase; MRT, mean residence time; MS, mass spectroscopy; NMP, 1-methylpyrrolidone; PD, pharmacodynamic; PDB, protein data bank; PK, pharmacokinetic; SAR, structure−activity relationships; SCC, squamous cell carcinoma; SD, solid dispersion; ±SD, standard deviation; SPR, surface plasmon resonance; TFAA, trifluoroacetic anhydride; TLC, thin-layer chromatography; VDss, steady state volume of distribution; VEGF, vascular endothelial growth factor; VEGFR2, vascular endothelial growth factor receptor 2; wt, wild-type

REFERENCES

(1) Maurer, G.; Tarkowski, B.; Baccarini, M. Raf kinases in cancer-roles and therapeutic opportunities. *Oncogene* **2011**, *30*, 3477−3488.

(2) Bollag, G.; Hirth, P.; Tsai, J.; Zhang, J.; Ibrahim, P. N.; Cho, H.; Spevak, W.; Zhang, C.; Zhang, Y.; Habets, G.; Burton, E. A.; Wong, B.; Tsang, G.; West, B. L.; Powell, B.; Shellooe, R.; Marimuthu, A.; Nguyen, H.; Zhang, K. Y. J.; Artis, D. R.; Schlessinger, J.; Su, F.; Higgins, B.; Iyer, R.; D'Andrea, K.; Koehler, A.; Stumm, M.; Lin, P. S.; Lee, R. J.; Grippo, J.; Puzanov, I.; Kim, K. B.; Ribas, A.; McArthur, G. A.; Sosman, J. A.; Chapman, P. B.; Flaherty, K. T.; Xu, X.; Nathanson, K. L.; Nolop, K. Clinical efficacy of a RAF inhibitor needs broad target blockade in BRAF-mutant melanoma. *Nature* **2010**, *467*, 596−599.

(3) Chapman, P. B.; Hauschild, A.; Robert, C.; Haanen, J. B.; Ascierto, P.; Larkin, J.; Dummer, R.; Garbe, C.; Testori, A.; Maio, M.; Hogg, D.; Lorigan, P.; Lebbe, C.; Jouary, T.; Schadendorf, D.; Ribas, A.; O'Day, S. J.; Sosman, J. A.; Kirkwood, J. M.; Eggermont, A. M. M.; Dreno, B.; Nolop, K.; Li, J.; Nelson, B.; Hou, J.; Lee, R. J.; Flaherty, K. T.; McArthur, G. A. For the BRIM-3 Study Group. Improved survival with Vemurafenib in melanoma with BRAF V600E mutation. *N. Engl. J. Med.* **2011**, *364*, 2507−2516.

(4) Ribas, A.; Flaherty, K. T. BRAF targeted therapy changes the treatment paradigm in melanoma. *Nat. Rev. Clin. Oncol.* **2011**, *8*, 426−433.

(5) Hauschild, A.; Grob, J. J.; Demidov, L. V.; Jouary, T.; Gutzmer, R.; Millward, M.; Rutkowski, P.; Blank, C. U.; Miller, W. H.; Kaempgen, E., Jr.; Martín-Algarra, S.; Karaszewska, B.; Mauch, C.; Chiarion-Sileni, V.; Martin, A. M.; Swann, S.; Haney, P.; Mirakhur, B.; Guckert, M. E.; Goodman, V.; Chapman, P. B. Dabrafenib in BRAF-mutated metastatic melanoma: a multicentre, open-label, phase 3 randomised controlled trial. *Lancet* **2012**, *380*, 358−365.

(6) Flaherty, K. T.; Puzanov, I.; Kim, K. B.; Ribas, A.; McArthur, G. A.; Sosman, J. A.; O'Dwyer, P. J.; Lee, R. J.; Grippo, J. F.; Nolop, K.; Chapman, P. B. Inhibition of mutated, activated BRAF in metastatic melanoma. *N. Engl. J. Med.* **2010**, *363*, 809−819.

(7) Anforth, R. M.; Blumetti, T. C. M. P.; Kefford, R. F.; Sharma, R.; Scolyer, R. A.; Kossard, S.; Long, G. V.; Fernandez-Peñas, P. Cutaneous manifestations of dabrafenib (GSK2118436): a selective inhibitor of mutant BRAF in patients with metastatic melanoma. *Br. J. Dermatol.* **2012**, *167*, 1153−1160.

(8) Falchook, G. S.; Long, G. V.; Kurzrock, R.; Kim, K. B.; Arkenau, T. H.; Brown, M. P.; Hamid, O.; Infante, J. R.; Millward, M.; Pavlick, A. C.; O'Day, S. J.; Blackman, S. C.; Curtis, C. M.; Lebowitz, P.; Ma, B.; Ouellet, D.; Kefford, R. F. Dabrafenib in patients with melanoma, untreated brain metastases, and other solid tumours: a phase 1 dose-escalation trial. *Lancet* **2012**, *379* (9829), 1893−1901.

(9) Hall-Jackson, C. A.; Eyers, P. A.; Cohen, P.; Goedert, M.; Boyle, F. T.; Hewitt, N.; Plant, H.; Hedge, P. Paradoxical activation of Raf by a novel Raf inhibitor. *Chem. Biol.* **1999**, *6*, 559−568.

(10) Poulikakos, P. I.; Zhang, C.; Bollag, G.; Shokat, K. M.; Rosen, N. RAF inhibitors transactivate RAF dimers and ERK signalling in cells with wild-type BRAF. *Nature* **2010**, *464*, 427−430.

(11) Su, F.; Viros, A.; Milagre, C.; Trunzer, K.; Bollag, G.; Spleiss, O.; Reis-Filho, J. S.; Kong, X.; Koya, R. C.; Flaherty, K. T.; Chapman, P. B.; Kim, M. J.; Hayward, R.; Martin, M.; Yang, H.; Wang, Q.; Hilton, H.; Hang, J. S.; Noe, J.; Lambros, M.; Geyer, F.; Dhomen, N.; Niculescu-Duvaz, I.; Zambon, A.; Niculescu-Duvaz, D.; Preece, N.; Robert, L.; Otte, N. J.; Mok, S.; Kee, D.; Ma, Y.; Zhang, C.; Habets, G.; Burton, E. A.; Wong, B.; Nguyen, H.; Kockx, M.; Andries, L.; Lestini, B.; Nolop, K. B.; Lee, R. J.; Joe, A. K.; Troy, J. L.; Gonzalez, R.; Hutson, T. E.; Puzanov, I.; Chmielowski, B.; Springer, C. J.; McArthur, G. A.; Sosman, J. A.; Lo, R. S.; Ribas, A.; Marais, R. RAS mutations in cutaneous squamous-cell carcinomas in patients treated with BRAF inhibitors. *N. Engl. J. Med.* **2012**, *366* (3), 207−215.

(12) Hatzivassiliou, G.; Song, K.; Yen, I.; Brandhuber, B. J.; Anderson, D. J.; Alvarado, R.; Ludlam, M. J.; Stokoe, D.; Gloor, S. L.; Vigers, G.; Morales, T.; Aliagas, I.; Liu, B.; Sideris, S.; Hoeflich, K. P.; Jaiswal, B. S.; Seshagiri, S.; Koeppen, H.; Belvin, M.; Friedman, L. S.; Malek, S. RAF inhibitors prime wild-type RAF to activate the MAPK pathway and enhance growth. *Nature* **2010**, *464* (7287), 431−435.

(13) Heidorn, S. J.; Milagre, C.; Whittaker, S.; Nourry, A.; Niculescu-Duvas, I.; Dhomen, N.; Hussain, J.; Reis-Filho, J. S.; Springer, C. J.; Pritchard, C.; Marais, R. Kinase-dead BRAF and oncogenic RAS cooperate to drive tumor progression through CRAF. *Cell* **2010**, *140* (2), 209−221.

(14) Yang, H.; Higgins, B.; Kolinsky, K.; Packman, K.; Go, Z.; Iyer, R.; Kolis, S.; Zhao, S.; Lee, R.; Grippo, J. F.; Schostack, K.; Simcox, M.

E.; Heimbrook, D.; Bollag, G.; Su, F. RG7204 (PLX4032), a selective BRAFV600E inhibitor, displays potent antitumor activity in preclinical melanoma models. *Cancer Res.* **2010**, *70*, 5518−5527.
(15) Okaniwa, M.; Hirose, M.; Imada, T.; Ohashi, T.; Hayashi, Y.; Miyazaki, T.; Arita, T.; Yabuki, M.; Kakoi, K.; Kato, J.; Takagi, T.; Kawamoto, T.; Yao, S.; Sumita, A.; Tsutsumi, S.; Tottori, T.; Oki, H.; Sang, B. -C.; Yano, J.; Aertgeerts, K.; Yoshida, S.; Ishikawa, T. Design and synthesis of novel DFG-out RAF/vascular endothelial growth factor receptor 2 (VEGFR2) inhibitors. 1. Exploration of [5,6]-fused bicyclic scaffolds. *J. Med. Chem.* **2012**, *55*, 3452−3478.
(16) Okaniwa, M.; Imada, T.; Ohashi, T.; Miyazaki, T.; Arita, T.; Yabuki, M.; Sumita, A.; Tsutsumi, S.; Higashikawa, K.; Takagi, T.; Kawamoto, T.; Inui, Y.; Yoshida, S.; Ishikawa, T. Design and synthesis of novel DFG-out RAF/vascular endothelial growth factor receptor 2 (VEGFR2) inhibitors: 2. Synthesis and characterization of a novel imide-type prodrug for improving oral absorption. *Bioorg. Med. Chem.* **2012**, *20*, 4680−4692.
(17) Hirose, M.; Okaniwa, M.; Miyazaki, T.; Imada, T.; Ohashi, T.; Tanaka, Y.; Arita, T.; Yabuki, M.; Kawamoto, T.; Tsutsumi, S.; Sumita, A.; Takagi, T.; Sang, B. C.; Yano, J.; Aertgeerts, K.; Yoshida, S.; Ishikawa, T. Design and synthesis of novel DFG-out RAF/vascular endothelial growth factor receptor 2 (VEGFR2) inhibitors: 3. Evaluation of 5-amino-linked thiazolo[5,4-*d*]pyrimidine and thiazolo-[5,4-*b*]pyridine derivatives. *Bioorg. Med. Chem.* **2012**, *20*, 5600−5615.
(18) For BRAF, DOI: 10.2210/pdb4dbn/pdb. For VEGFR2, DOI:10.2210/pdb3vnt/pdb.
(19) Kaufmann, H. P.; Weber, E. Arzneimittelsynthetische studien IV. Synthese schwefelhaltiger verbindungen. *Arch. Pharm.* **1929**, 192−211.
(20) Stuckwisch, C. G. Derivatives of 2-amino-6-methoxybenzothiazole. *J. Am. Chem. Soc.* **1949**, *71*, 3417.
(21) Ismail, I. A.; Sharp, D. E.; Chedekel, M. R. Synthesis of benzothiazoles. α-Amino-(4-hydroxy-6-benzothiazolyl)propionic acid. *J. Org. Chem.* **1980**, *45*, 2243−2246.
(22) Charris, J.; Monasterios, M.; Dominguez, J.; Infante, W.; De Castro, N. Synthesis of some 5-nitro-2-furfurylidene derivatives and their antibacterial and antifungal activities. *Heterocycl. Commun.* **2002**, *8* (3), 275−280.
(23) Tomasi, A.; Morgan, B. P.; McDonald, A.; Roof, D.; Maxon, M. Compounds, Compositions, and Methods. WIPO Patent Application WO 2004/098494, Nov 18, 2004.
(24) Malik, J. K.; Manvi, F. V.; Nanjwade, B. K.; Singh, S. Synthesis and screening of some new 2-amino substituted-benzothiazole derivatives for antifungal activity. *Drug Invention Today* **2009**, *1* (1), 32−34.
(25) Schnur, R. C.; Fliri, A. F. J.; Kajiji, S.; Pollack, V. A. *N*-(5-fluorobenzothiazol-2-yl)-2-guanidinothiazole-4-carboxamide. A novel, systemically active antitumor agent effective against 3LL Lewis Lung carcinoma. *J. Med. Chem.* **1991**, *34*, 914−918.
(26) Wang, M.; Gao, M.; Mock, B. H.; Miller, K. D.; Sledge, G. W.; Hutchins, G. D.; Zheng, Q. H. Synthesis of carbon-11 labeled fluorinated 2-arylbenzothiazoles as novel potential PET cancer imaging agents. *Bioorg. Med. Chem.* **2006**, *14* (24), 8599−8607.
(27) Wang, M.; Jiang, S.; Hou X. [1,2,3] Piazthiole-7-formhydrazide Derivative as I-Type Plant Disease-Resisting Revulsive. SIPO Patent Application CN 1389114, Jan 08, 2003.
(28) Gyorkos, A. C.; Corrette, C. P.; Cho, S. Y.; Turner, T. M.; Pratt, S. A.; Aso, K.; Kori, M.; Gyoten, M. Preparation of Nitrogen-Containing Fused Heterocyclic Compounds Like Benzimidazoles and Benzothiazoles as CRF Receptor Antagonists. WIPO Patent Application WO 2005/044793, May 19, 2005.
(29) The coordinates and structure factors have been deposited with the Protein Data Bank with accession code 4KSP for BRAF with **8B**.
(30) Bondi, A. van der Waals volumes and radii. *J. Phys. Chem.* **1964**, *68*, 441−451.
(31) The coordinates and structure factors have been deposited with the Protein Data Bank with accession code 4KSQ for BRAF with **5B**.
(32) Brameld, K. A.; Kuhn, B.; Reuter, D. C.; Stahl, M. Small molecule conformational preferences derived from crystal structure data. A medicinal chemistry focused analysis. *J. Chem. Inf. Model.* **2008**, *48* (1), 1−24.
(33) Tsai, J.; Lee, J. T.; Wang, W.; Zhang, J.; Cho, H.; Mamo, S.; Bremer, R.; Gillette, S.; Kong, J.; Haass, N. K.; Sproesser, K.; Li, L.; Smalley, K. S.; Fong, D.; Zhu, Y. L.; Marimuthu, A.; Nguyen, H.; Lam, B.; Liu, J.; Cheung, I.; Rice, J.; Suzuki, Y.; Luu, C.; Settachatgul, C.; Shellooe, R.; Cantwell, J.; Kim, S. H.; Schlessinger, J.; Zhang, K. Y.; West, B. L.; Powell, B.; Habets, G.; Zhang, C.; Ibrahim, P. N.; Hirth, P.; Artis, D. R.; Herlyn, M.; Bollag, G. Discovery of a selective inhibitor of oncogenic B-Raf kinase with potent antimelanoma activity. *Proc. Natl. Acad. Sci. U.S.A.* **2008**, *105*, 3041−3046.
(34) Wood, E. R.; Truesdale, A. T.; McDonald, O. B.; Yuan, D.; Hassell, A.; Dickerson, S. H.; Ellis, B.; Pennisi, C.; Horne, E.; Lackey, K.; Alligood, K. J.; Rusnak, D. W.; Gilmer, T. M.; Shewchuk, L. Aunique structure for epidermal growth factor receptor bound to GW572016 (Lapatinib): relationships among protein conformation, inhibitor off-rate, and receptor activity in tumor cells. *Cancer Res.* **2004**, *64*, 6652−6659.
(35) Iwata, H.; Imamura, S.; Hori, A.; Hixon, M. S.; Kimura, H.; Miki, H. Biochemical characterization of TAK-593, a novel VEGFR/PDGFR inhibitor with a two-step slow binding mechanism. *Biochemistry* **2011**, *50*, 738−751.
(36) Copeland, R. A.; Pompliano, D. L.; Meek, T. D. Drug-target residence time and its implications for lead optimization. *Nat. Rev. Drug Discovery* **2006**, *5* (9), 730−739.
(37) The Ministry of Health, Labour and Welfare. The Ministry of Health, Labour and Welfare Ministerial Notification No. 285. General Tests/Reagents, Test Solutions. *The Japanese Pharmacopoeia*, English version, Ministry of Health, Labour and Welfare: Tokyo, Japan, 2006; Vol. *15*, p. 239.
(38) Lavoie, H.; Thevakumaran, N.; Gavory, G.; Li, J. J.; Padeganeh, A.; Guiral, S.; Duchaine, J.; Mao, D. Y. L.; Bouvier, M.; Sicheri, F.; Therrien, M. Inhibitors that stabilize a closed RAF kinase domain conformation induce dimerization. *Nat. Chem. Biol.* **2013**, *9* (7), 428−436.
(39) Carnahan, J.; Beltran, P. J.; Babij, C.; Le, Q.; Rose, M. J.; Vonderfecht, S.; Kim, J. L.; Smith, A. L.; Nagapudi, K.; Broome, M. A.; Fernando, M.; Kha, H.; Belmontes, B.; Radinsky, R.; Kendall, R.; Burgess, T. L. Selective and potent Raf inhibitors paradoxically stimulate normal cell proliferation and tumor growth. *Mol. Cancer Ther.* **2010**, *9*, 2399−2410.
(40) Galvin, K. *MLN2480: A Novel pan-RAF Inhibitor for Treatment of BRAF Mutant and Wild-Type Tumors*, 103rd Annual Meeting of American Association for Cancer Research (AACR), Chicago, IL, Mar 31−Apr 4, 2012; Abstract.